ADAMTS-7 Inhibits Re-endothelialization of Injured Arteries and Promotes Vascular Remodeling Through Cleavage of Thrombospondin-1

Thorsten Kessler, MD*; Lu Zhang, PhD*; Ziyi Liu, PhD; Xiaoke Yin, PhD; Yaqian Huang, PhD; Yingbao Wang, BS; Yi Fu, PhD; Manuel Mayr, MD, PhD; Qing Ge, MD, PhD; Qingbo Xu, MD, PhD; Yi Zhu, MD; Xian Wang, MD, PhD; German Mouse Clinic Consortium†; Kjestine Schmidt, PhD; Cor de Wit, MD; Jeanette Erdmann, PhD; Heribert Schunkert, MD; Zouhair Aherrahrou, PhD‡; Wei Kong, MD, PhD‡

Background—ADAMTS-7, a member of the disintegrin and metalloproteinase with thrombospondin motifs (ADAMTS) family, was recently identified to be significantly associated genomewide with coronary artery disease. However, the mechanisms that link ADAMTS-7 and coronary artery disease risk remain elusive. We have previously demonstrated that ADAMTS-7 promotes vascular smooth muscle cell migration and postinjury neointima formation via degradation of a matrix protein cartilage oligomeric matrix protein. Because delayed endothelium repair renders neointima and atherosclerosis plaque formation after vessel injury, we examined whether ADAMTS-7 also inhibits re-endothelialization.

Methods and Results—Wire injury of the carotid artery and Evans blue staining were performed in *Adamts7*$^{-/-}$ and wild-type mice. *Adamts*-7 deficiency greatly promoted re-endothelialization at 3, 5, and 7 days after injury. Consequently, *Adamts*-7 deficiency substantially ameliorated neointima formation in mice at days 14 and 28 after injury in comparison with the wild type. In vitro studies further indicated that ADAMTS-7 inhibited both endothelial cell proliferation and migration. Surprisingly, cartilage oligomeric matrix protein deficiency did not affect endothelial cell proliferation/migration and re-endothelialization in mice. In a further examination of other potential vascular substrates of ADAMTS-7, a label-free liquid chromatography-tandem mass spectrometry secretome analysis revealed thrombospondin-1 as a potential ADAMTS-7 target. The subsequent studies showed that ADAMTS-7 was directly associated with thrombospondin-1 by its C terminus and degraded thrombospondin-1 in vivo and in vitro. The inhibitory effect of ADAMTS-7 on postinjury endothelium recovery was circumvented in *Tsp1*$^{-/-}$ mice.

Conclusions—Our study revealed a novel mechanism by which ADAMTS-7 affects neointima formation. Thus, ADAMTS-7 is a promising treatment target for postinjury vascular intima hyperplasia. **(*Circulation*. 2015;131:1191-1201. DOI: 10.1161/CIRCULATIONAHA.114.014072.)**

Key Words: matrix metalloproteinases ■ neointima ■ vascular remodeling

Endothelial cells (ECs) play an essential role in the modulation of vascular homeostasis. During aging and specifically during the development of atherosclerosis, ECs are exposed to various damaging stimuli and are thereby prone to injury.[1] Rapid endothelial recovery, or re-endothelialization, correlates with diminished plaque formation.[2] Likewise, coronary intervention–induced vascular injury requires an

Editorial see p 1156
Clinical Perspective on p 1201

Received July 16, 2014; accepted January 16, 2015.

From Deutsches Herzzentrum München, Klinik für Herz- und Kreislauferkrankungen, Technische Universität München, Germany (T.K., H.S.); Department of Physiology and Pathophysiology, School of Basic Medical Sciences, Peking University, Beijing, China (L.Z., Z.L., Y.H., Y.W., Y.F., X.W., W.K.); Key Laboratory of Molecular Cardiovascular Science, Ministry of Education, Beijing, China (L.Z., Z.L., Y.H., Y.W., Y.F., X.W., W.K.); Cardiovascular Division, Kings College London BHF Centre, United Kingdom (X.Y., M.M., Q.X.); Department of Immunology, School of Basic Medical Sciences, Peking University, Beijing, China (Q.G.); School of Basic Medical Sciences, Tianjin University, Beijing, China (Y.Z.); Institut für Physiologie, Universität zu Lübeck, Germany (K.S., C.d.W.); Deutsches Zentrum für Herz-Kreislauf-Forschung (DZHK) e.V. (German Center for Cardiovascular Research), partner site Hamburg/Kiel/Lübeck, Lübeck, Germany (K.S., C.d.W., J.E., Z.A.); Institut für Integrative und Experimentelle Genomik, Universität zu Lübeck, Germany (J.E., Z.A.); and Deutsches Zentrum für Herz-Kreislauf-Forschung (DZHK) e.V. (German Center for Cardiovascular Research), partner site Munich Heart Alliance (MHA), München, Germany (H.S.).

*Drs Kessler and Zhang contributed equally.

†The members of the German Mouse Clinic Consortium are listed in the online-only Data Supplement.

‡Drs Aherrahrou and Kong contributed equally.

The online-only Data Supplement is available with this article at http://circ.ahajournals.org/lookup/suppl/doi:10.1161/CIRCULATIONAHA.114.014072/-/DC1.

Correspondence to Wei Kong, MD, PhD, Department of Physiology and Pathophysiology, Basic Medical College of Peking University, Beijing 100191, People's Republic of China. E-mail kongw@bjmu.edu.cn; and Zouhair Aherrahrou, PhD, Institut für Integrative und Experimentelle Genomik, Universität zu Lübeck, Maria-Goeppert-Str. 1, 23562 Lübeck, Germany. E-mail zouhair.aherrahrou@iieg.uni-luebeck.de

efficient re-endothelialization to prevent postinjury restenosis and thrombotic events. The rate of luminal endothelial repair is thus a critical modulator of arterial lesion formation after injury. Drug-eluting stents have failed to improve the long-term prognosis and increased the stent thrombosis rate,[3–5] potentially because they inhibit not only vascular smooth muscle cell (VSMC) proliferation/migration, but also re-endothelialization.[6,7] Therefore, new strategies that aim to promote endothelial recovery, and simultaneously inhibit VSMC activation, as well, are needed for the effective prevention and treatment of atherosclerosis and postinjury restenosis.

Metalloproteinases are critical in vascular wall remodeling through matrix or nonmatrix degradation.[8] Recently, we described ADAMTS-7, a member of a disintegrin and metalloproteinase with thrombospondin motifs (ADAMTS) family, in the mediation of VSMC migration and the promotion of neointima formation following artery injury through the degradation of cartilage oligomeric matrix protein (COMP).[9,10] To date, COMP is the only identified substrate of ADAMTS-7 in the vessel wall and is believed to mediate its functional effects.[11,12] Three recent genomewide association studies have further revealed ADAMTS-7 as a novel locus associated with human coronary atherosclerosis.[13–15] A nonsynonymous single-nucleotide polymorphism in the prodomain of ADAMTS-7 is inversely related to VSMC migration, COMP cleavage, and the prevalence of atherosclerosis.[16] Moreover, ADAMTS-7 promotes VSMC and aortic calcification by disturbing the balance between osteogenic bone morphogenetic protein 2 and its natural inhibitor COMP.[12,17] However, the underlying mechanism of ADAMTS-7 in atherogenesis and postinjury vascular remodeling remains elusive. In this current study, we report that ADAMTS-7 not only promotes VSMC activation, but also inhibits postinjury endothelial cell recovery via a COMP-independent mechanism.

Methods

All animal studies followed the guidelines of the Animal Care and Use Committees of Peking University, People's Republic of China, and Schleswig-Holstein and Bavaria, Germany. The *Adamts7* gene was interrupted by introducing an internal ribosome entry site followed by the β-galactosidase sequence between exons 4 and 5. Wire injury of the mouse carotid artery was performed in 12-week-old male mice as described.[18] Gel-liquid chromatography-mass spectrometry analysis of secretome was performed as described.[19] An expanded and detailed Materials and Methods section is available in the online-only Data Supplement.

Results

Adamts7$^{-/-}$ Mice Are Viable and Do Not Show Any Obvious Phenotype

The *Adamts7* gene was interrupted by the introduction of an internal ribosome entry site followed by the β-galactosidase sequence between exons 4 and 5 (Figure 1A). Interruption of the gene was visualized by polymerase chain reaction on genomic DNA and reverse transcription polymerase chain reaction on mRNA from heart, kidney, and liver tissues (Figure 1B and 1C). Correct introduction of the β-galactosidase sequence was verified by X-gal staining of heart tissue (Figure 1D).

Large-Scale Phenotyping of *Adamts7*$^{-/-}$ Mice

Male and female *Adamts7*$^{-/-}$ mice were fertile and segregated with the assumed Mendelian frequencies. Wild-type (WT) and *Adamts7*$^{-/-}$ mice were subjected to a large-scale phenotyping as previously described.[20] As shown in Tables I through IV in the online-only Data Supplement, aside from changes in anxiety-related behavior, *Adamts7*$^{-/-}$ mice did not display abnormal phenotypes measured by vital parameters, echocardiographic analysis, severe organ dysfunction, or histopathologic abnormalities. Lung function analysis revealed increased lung function parameters and reduced resistance. However, histopathologic analysis did not detect emphysema (data not shown). We did find some sex-specific effects, in particular, on energy metabolism (Table II in the online-only Data Supplement). However, without a proatherogenic background, *Adamts7*$^{-/-}$ mice did not display changes in blood lipid levels after 15 weeks of Western diet in comparison with WT mice (Table IV in the online-only Data Supplement).

ADAMTS-7 Deficiency Promotes Re-endothelialization and Ameliorates Neointima Formation in Wire-Injured Mouse Carotid Arteries

To test the hypothesis concerning if ADAMTS-7 is involved in postinjury endothelium recovery, we performed wire injury in the carotid artery of *Adamts7*$^{-/-}$ mice and littermate WT C57/BL6 mice. Re-endothelialization was quantified by en face Evans blue staining of the denuded area at 3, 5, and 7 days after injury (Figure 1E). WT ECs were severely damaged immediately after injury and recovered by ≈25% at day 3, 45% at day 5, and 65% at day 7. In contrast, re-endothelialization in *Adamts7*$^{-/-}$ mice was 50% at day 3, 75% at day 5, and 85% at day 7 postinjury. Subsequent neointimal hyperplasia was completely abolished in *Adamts7*$^{-/-}$ mice at 14 and 28 days. Of note, media area and circumference of external elastic lamina did not differ between the 2 groups (Figure 1F).

ADAMTS-7 Inhibits EC Proliferation In Vivo and In Vitro

Next, we examined whether ADAMTS-7 affects EC proliferation. In vivo proliferation was assessed by bromodeoxyuridine incorporation. ECs were identified by en face immunofluorescence staining of von Willebrand Factor. The bromodeoxyuridine-positive cells by en face staining reflected proliferating cells at the wound margins proximal to the impaired artery. EC proliferation was significantly enhanced in *Adamts7*$^{-/-}$ mice in comparison with WT mice 3 days after injury (Figure 2A).

Next, we monitored human umbilical vein endothelial cell (HUVEC) proliferation in vitro. Ectopic expression of ADAMTS-7 by adenovirus (Ad-*ADAMTS-7*) at 10 multiplicities of infection markedly repressed HUVEC proliferation as evidenced by cell counting via kit-8 (CCK-8), by cell cycle analysis via flow cytometry, and cell cycle checkpoint protein measurement by Western Blot (Figure 2B through 2D). A neutralizing antibody that targeted the metalloproteinase domain of ADAMTS-7 was applied and functionally characterized. The antibody circumvented the COMP degradation capacity of ADAMTS-7 in a dose-dependent manner (Figure IA in the online-only Data Supplement), and ADAMTS-7–induced VSMC migration, as well (Figure

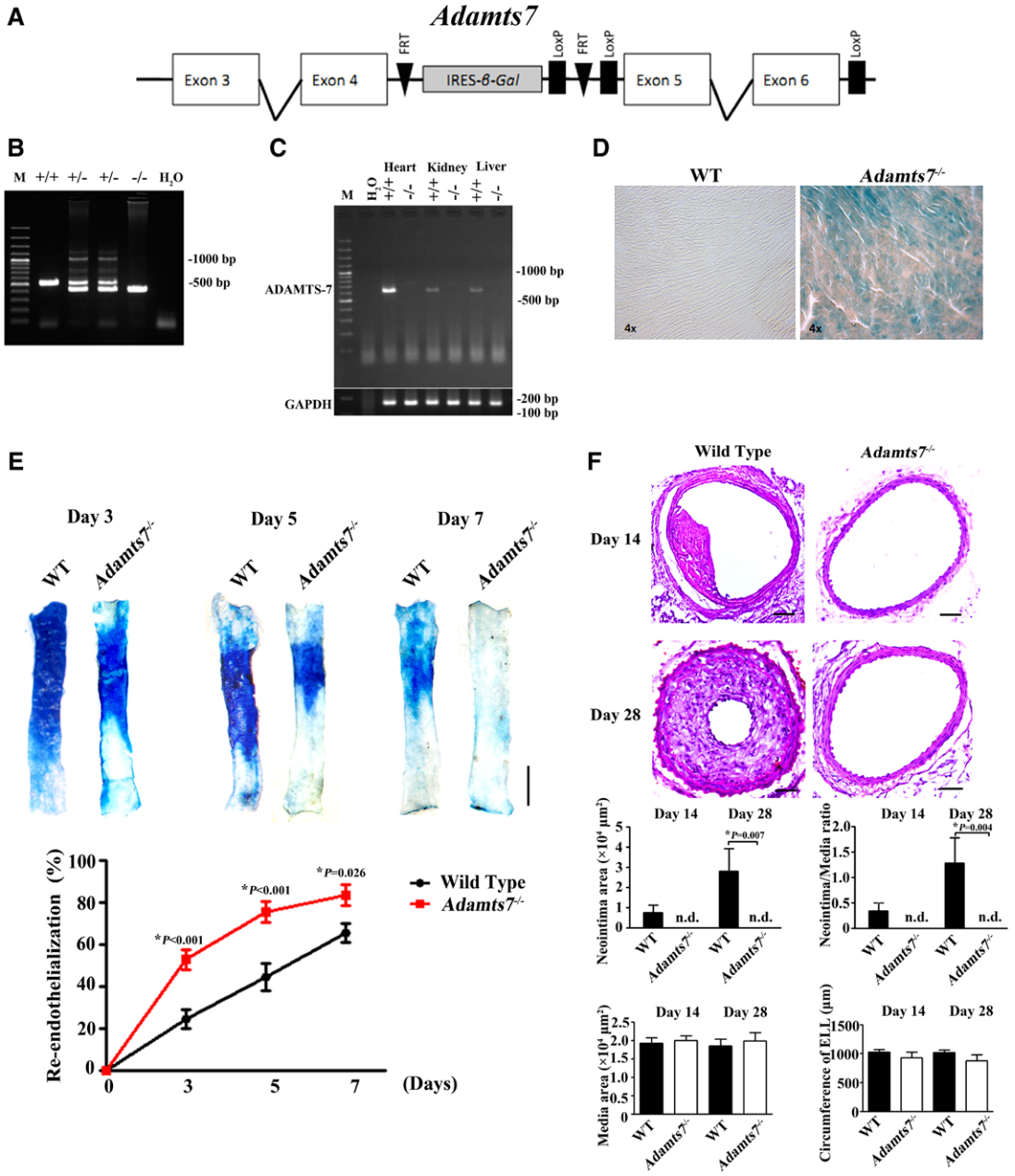

Figure 1. Adamts-7 deficiency promotes re-endothelialization and ameliorates neointima formation in wire-injured mice carotid arteries. **A**, Targeting vector for genomic deletion of *Adamts7*. *Adamts7*$^{-/-}$ embryonic stem cells were used to generate *Adamts7*$^{-/-}$ mice by the insertion of an internal ribosome entry site followed by the β-galactosidase sequence and a neomycin cassette (trans-NIH Knock-Out Mouse Project, KOMP Repository, USA).[19a] **B**, Genomic PCR results of the *Adamts7*$^{-/-}$ mice. **C**, *Adamts7* gene expression in heart, kidney, and liver. **D**, Representative pictures of β-galactosidase staining of heart tissue. **E**, Re-endothelialization was quantified in Evans blue–stained carotid arteries at 3, 5, and 7 days after vascular injury (representative pictures). Blue staining indicates endothelial denudation. Scale bar, 1 mm, **P*<0.05 vs wild type (n=6–8 for each group). **F**, Neointima formation was determined on hematoxylin and eosin–stained cross sections of carotid arteries 14 and 28 days after vascular wire injury (n=6 each group). Scale bar, 100 μm. **P*<0.05. ELL indicates external elastic lamina; n.d., not detectable; PCR, polymerase chain reaction; and WT, wild type.

IB in the online-only Data Supplement). Interestingly, the ADAMTS-7 neutralizing antibody dose-dependently reversed the inhibitory effect of ADAMTS-7 on EC proliferation (Figure 2E). These data reinforced that ADAMTS-7 specifically targets EC proliferation.

ADAMTS-7 Represses EC Migration

Because cell migration is an essential step in the re-endothelialization response, we assessed the effects of ADAMTS-7 on EC migratory ability. An in vitro scratch-wound assay revealed reduced migration of Ad-*ADAMTS-7*–infected HUVECs in comparison with Ad-*LacZ*–infected cells. The mean migration distance was shorter than with the control cells by 48%, 32%, and 43% at 12, 18, and 24 hours after injury, respectively (Figure 3A). Additionally, modified Boyden chamber assays were performed. A dramatic decrease of migration was observed in Ad-*ADAMTS-7*–infected HUVECs in comparison with Ad-*LacZ*–infected cells (Figure 3B). Reciprocally,

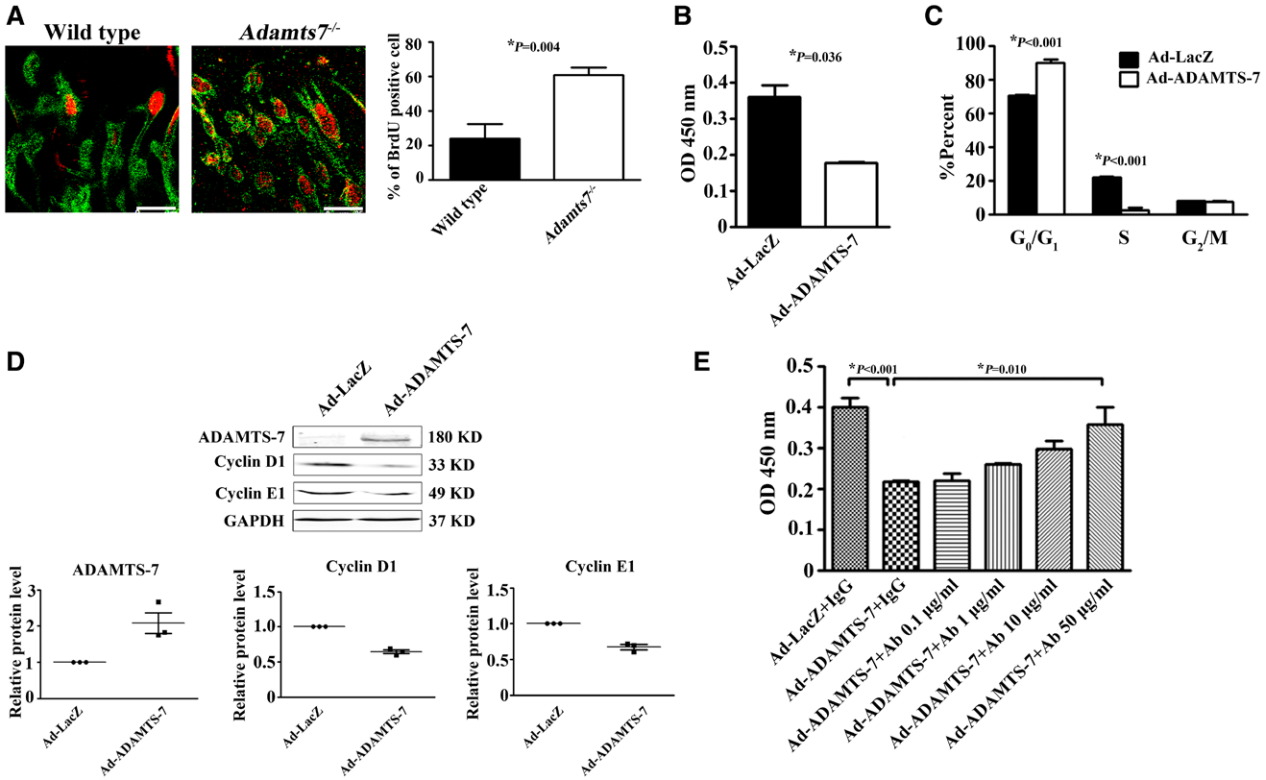

Figure 2. ADAMTS-7 inhibits HUVEC proliferation in vivo and in vitro. **A**, Representative BrdU-positive endothelial cells at the endothelial wound margins in carotid arteries 3 days after vascular injury. Proliferating nuclei were indicated by BrdU incorporation (red), and endothelial cells were indicated by vWF staining (green, n=3 each group). Scale bar, 50 μm. **B**, Proliferation of HUVECs infected with Ad-*ADAMTS-7* or Ad-*LacZ* was determined by Cell Counting Kit-8 (CCK-8). Results are means±SEM from 3 independent experiments performed in duplicate. **C**, Cell-cycle distribution of HUVECs was confirmed by propidium iodide staining and FACS analysis. Results are means±SEM from 3 independent experiments performed in duplicate. **D**, Representative Western blot of cell-cycle checkpoint protein in Ad-*ADAMTS-7* and Ad-*LacZ*–infected HUVECs. Bar represents means±SEM from 3 independent experiments. **E**, ADAMTS-7 inhibition by neutralization antibody abolished the antiproliferation effect. HUVECs were supplemented with ADAMTS-7 neutralization antibody (0.1–50 μg/mL) in culture medium when infected with adenovirus. Results are means±SEM from 4 independent experiments performed in duplicate. BrdU indicates bromodeoxyuridine; FACS, fluorescence-activated cell sorting; HUVEC, human umbilical vein endothelial cell; IgG, immunoglobulin G; SEM, standard error of the mean; and vWF, von Willebrand Factor.

ADAMTS-7 inhibition by neutralization antibody significantly abolished the antimigratory effect of ADAMTS-7 (Figure 3C).

COMP Does Not Affect EC Proliferation/Migration

Our previous studies have shown that ADAMTS-7 directly binds to and degrades COMP in VSMCs and injured vessels and subsequently promotes VSMC migration.[9,10] A recent study also revealed that an ADAMTS-7 single-nucleotide polymorphism alters COMP degradation and VSMC migration and therefore affects coronary artery disease risk.[14] Because COMP is primarily expressed in VSMCs but not in ECs,[21] we then examined whether COMP also affects re-endothelialization. Thus, HUVECs were supplemented with increasing amounts of purified COMP (concentration from 50 to 200 ng/mL) or cultured on plates coated with purified COMP. Interestingly, neither treatment affected HUVEC proliferation (Figure IIA and IIB in the online-only Data Supplement). In accordance, scratch-wound assays on HUVECs supplemented with various amounts of COMP revealed no difference in migration (Figure IIC in the online-only Data Supplement). To avoid the high level of mitogens masking the potential effects of COMP, the proliferation and migration of HUVECs were analyzed in the presence of 1% fetal bovine serum. Neither cell proliferation nor migration was influenced by increasing the amount of purified COMP (Figure IID and IIE in the online-only Data Supplement). Next, wire injury was conducted in *Comp*$^{-/-}$ and WT mice. In accordance, re-endothelialization was not significantly different between WT and *Comp*$^{-/-}$ mice (Figure IIF in the online-only Data Supplement). In contrast, the neointima area was greatly increased in *Comp*$^{-/-}$ mice 28 days after wire injury in comparison with littermate WT mice (Figure IIG in the online-only Data Supplement), reinforcing the notion that ADAMTS-7 retards endothelium repair independent of COMP. These data suggest that, although ADAMTS-7 promotes VSMC migration and neointima formation via COMP degradation, ADAMTS-7 may inhibit EC recovery via COMP-independent mechanisms.

Identification of a Novel Substrate for ADAMTS-7 by Secretome Analysis

To identify a novel substrate of ADAMTS-7 and reveal the mechanism of ADAMTS-7 on re-endothelialization, a secretome proteomics analysis was performed. Primary rat VSMCs were adenovirally infected with Ad-*ADAMTS-7* or control Ad-*GFP*. Supernatant was collected and analyzed

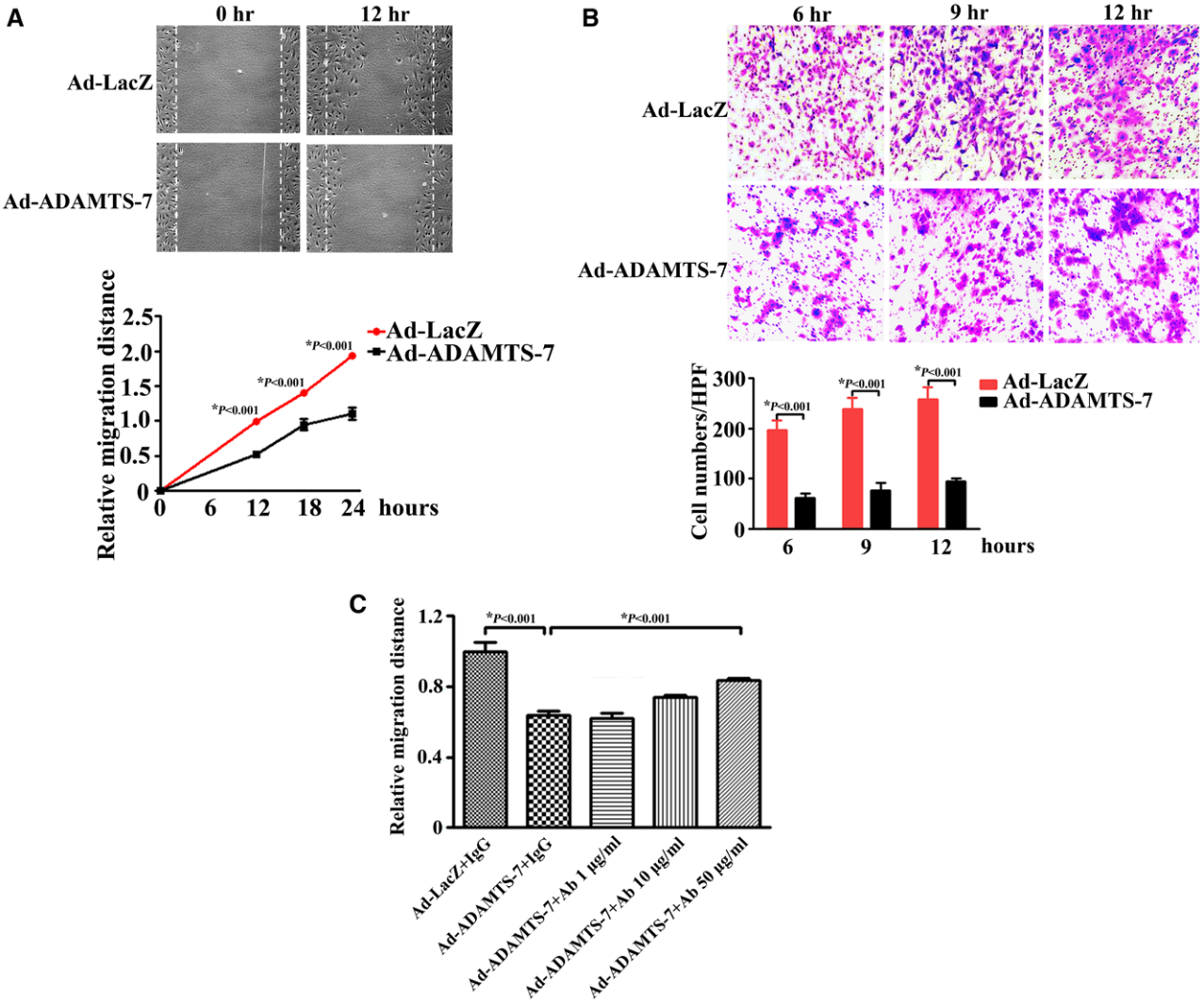

Figure 3. ADAMTS-7 suppresses HUVEC migratory ability in vitro. **A**, Representative images of cell migration 12 hours after scratching. Confluent HUVEC monolayers were scratch wounded 48 hours after adenoviral infection. The cells were maintained in culture for an additional 12, 18, and 24 hours before imaging (dotted line indicates wound edge). The mean distance migrated by the HUVECs was quantified (average of 4 independent microscope fields for 3 independent experiments each, magnification ×100). **B**, Representative images of modified Boyden chamber assay at 6, 9, and 12 hours (magnification ×100). Migrated cells were quantified by the average of 4 randomly chosen high-power fields (HPF) of 3 independent duplicate experiments. **C**, Neutralization antibody (1–50 μg/mL) rescued the suppressed migration in Ad-*ADAMTS-7*–infected HUVECs 12 hours after scratch. Results are means±SEM from 3 independent experiments. HUVEC indicates human umbilical vein endothelial cell; IgG, immunoglobulin G; and SEM, standard error of the mean.

by proteomics. As expected, ADAMTS-7 was dramatically increased. The gel-liquid chromatography-tandem mass spectrometry analysis identified 290 proteins in the conditioned media, of which 29 proteins were identified with significant differences ($P \leq 0.05$; Table V in the online-only Data Supplement). Among these, 13 proteins were extracellular proteins or plasma membrane proteins. These proteins included extracellular matrix proteins (thrombospondin-1, osteopontin, periostin, olfactomedin-like protein 3, growth/differentiation factor 6 and Sushi, von Willebrand factor type A, epidermal growth factor, and pentraxin domain–containing protein 1), cell proliferation regulators (pigment epithelium–derived factor and guanine nucleotide–binding protein subunit beta-2-like 1), peroxidases (thioredoxin), and cytoskeleton proteins (actin-related protein 3, elastin, moesin, and septin-11).

Thrombospondin-1 (TSP-1) is the first identified and potent endogenous antiangiogenic protein capable of inhibiting EC proliferation and migration and was of close to statistical significance ($P=0.0509$) regulated by ADAMTS-7 overexpression. Further enzyme-linked immunosorbent assay analysis confirmed the reduced secretion of TSP-1 in the supernatant of Ad-*ADAMTS-7* in comparison with Ad-*LacZ*–infected T/G HA VSMCs (Figure 4A). TSP-1 has been shown to be expressed and secreted by ECs.[22,23] Similarly, the secretion of endogenous TSP-1 from HUVECs was markedly reduced by Ad-*ADAMTS-7* infection in comparison with Ad-*LacZ* treatment (4.798±0.7136 versus 2.145±0.8099 ng/10^4 cells; n=8; $P<0.05$; Figure 4B). In addition, increased TSP-1 was detected in the aorta of *Adamts7*$^{-/-}$ mice, which indicates that ADAMTS-7 truly affects the TSP-1 level (Figure 4C).

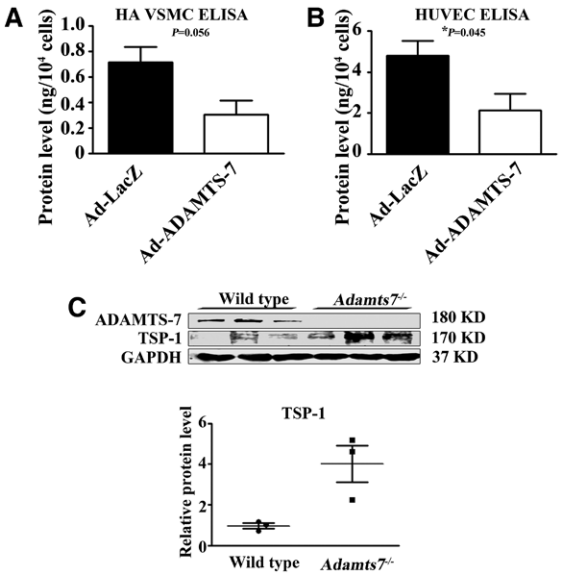

Figure 4. ADAMTS-7 decreases thrombospondin-1 expression at the protein level. **A**, Identification of the TSP-1 protein level in the culture medium of Ad-*lacZ*– or Ad-*ADAMTS-7*–infected T/G HA VSMC by ELISA analysis. Results are means±SEM from 5 independent experiments. **B**, Protein level of TSP-1 in HUVEC supernatant. Results are means±SEM from 8 independent experiments. **C**, Western blot analysis of TSP-1 expression in the aorta of *Adamts7*$^{-/-}$ mice. n=3. ELISA indicates enzyme-linked immunosorbent assay; HA, human aortic; HUVEC, human umbilical vein endothelial cell; IgG, immunoglobulin G; SEM, standard error of the mean; TSP-1, thrombospondin-1; and VSMC, vascular smooth muscle cell.

ADAMTS-7 Associates With TSP-1

Because protein-protein interactions are a fundamental process for most enzyme-substrate reactions, we first examined the interaction between ADAMTS-7 and TSP-1. The coimmunoprecipitation assay was conducted to verify the association of ADAMTS-7 and TSP-1 in vivo. In WT aorta, a specific TSP-1 band was present in the complex immunoprecipitated with anti–ADAMTS-7 antibody, but not with control immunoglobulin G. Accordantly, coimmunoprecipitation with anti–TSP-1 antibody revealed that TSP-1 also precipitated ADAMTS-7 (Figure 5A). In contrast, no protein interaction was detected in *Adamts7*$^{-/-}$ aorta. A specific interaction between ADAMTS-7 and TSP-1 was further confirmed in primary HUVECs, and COS-7 cells, as well, cotransfected with ADAMTS-7 and TSP-1 (Figure 5B and 5C). To further characterize the binding motif of ADAMTS-7 attributable to the TSP-1 interaction, a mammalian 2-hybrid assay was performed by cotransfecting Eahy 926 cells with the pACT plasmids that expressed various ADAMTS-7 deletion mutants and the pBIND plasmid that encoded the full-length TSP-1, respectively. The ADAMTS-7 prodomain (amino acids [aa] 26–246), the metalloproteinase plus disintegrin-like and cysteine-rich domain (aa 238–711), and the spacer-1 plus 3 TSP repeats (aa 703–1007) were not bound to TSP-1. Instead, the spacer-2 plus 4 C-terminal TSP repeats of ADAMTS-7 (aa 999–1595) bound to TSP-1 (Figure 5D). The interaction between the ADAMTS-7 C terminus and TSP-1 was also confirmed by coimmunoprecipitation with anti-Flag antibody in Eahy 926 cells transfected with Flag-CMV vectors that expressed various ADAMTS-7 deletion mutants (Figure 5E). Taken together, our data show that ADAMTS-7 binds to TSP-1 in vitro and in vivo.

ADAMTS-7 Degrades TSP-1 In Vitro

Next, we analyzed TSP-1 cleavage by ADAMTS-7 in HUVECs. Western blot analysis of Ad-*ADAMTS-7*– and Ad-*LacZ*–infected cells revealed reduced levels of full-length TSP-1 in both whole-cell lysate (Figure 6A) and supernatant (Figure 6B). Interestingly, a 140-kDa fragment was repeatedly observed in the supernatant, but not in the cell lysate. In contrast, the mRNA level of TSP-1 was not altered by ADAMTS-7 (Figure III in the online-only Data Supplement). To further verify the observation, COS-7 cells were infected with increasing amounts of adenoviral constructs that expressed LacZ and ADAMTS-7, respectively. The supernatant was collected, concentrated, and incubated with purified human TSP-1 at 37°C for 4 hours. With increased expression of ADAMTS-7, a gradually reduced level of full-length TSP-1 (170 kDa) was observed in parallel with an increased 140-kDa fragment (Figure 6C). Accordingly, an enhanced cleavage fragment of TSP-1 was observed with increasing amounts of extraneous TSP-1 (Figure 6D). This effect, however, was completely abolished by adding the ADAMTS-7–neutralizing antibody (Figure 6E). Previous studies have suggested that the catalytic domains of ADAMTS-7 and ADAMTS-20 produced in bacteria can digest their substrates in vitro.[9] Using a similar method, we purified the catalytic domain (aa 217–427) of rADAMTS-7 as a glutathione-*S*-transferase fusion protein in bacteria. The glutathione-*S*-transferase moiety was further removed by thrombin, and the purity of protein was confirmed by visualization using Coomassie staining (data not shown). The recombinant catalytic domain of ADAMTS-7 was incubated with purified human TSP-1 in a buffer containing 50 mmol/L Tris-HCl, 150 mmol/L NaCl, 5 mmol/L $CaCl_2$, 2 mmol/L $ZnCl_2$, and 0.05% Brij-35, pH 7.5. As shown in Figure 6F, the catalytic domain of ADAMTS-7 digested TSP-1 in a dose-dependent manner.

ADAMTS-7 Inhibits Re-endothelialization via TSP-1

We next examined whether ADAMTS-7 inhibited postinjury EC recovery via TSP-1. TSP-1 expression was specifically silenced by small interfering RNA treatment of HUVECs (Figure 7A). As shown in Figure 7B and 7C, the inhibitory effect of ADAMTS-7 on EC proliferation was significantly abolished in the absence of TSP-1 as evident by both cell counting and cell cycle analysis. In line with this observation, TSP-1 deficiency also circumvented the inhibitory effect of ADAMTS-7 on EC migration (Figure 7D). As a consequence, the retardation of re-endothelialization by ADAMTS-7 overexpression was circumvented in *Tsp1*$^{-/-}$ mice (Figure 7E), which indicates ADAMTS-7 refrains endothelial repair from repairing via TSP-1 (Figure 8).

Discussion

Aberrant EC recovery is inversely related to neointima formation during atherosclerosis and postinjury restenosis. Our current study revealed ADAMTS-7 as a potent inhibitor of endothelial recovery in response to injury. Using *Adamts7*$^{-/-}$ mice and injury models, we uncovered that, in addition to the suppression of VSMC migration, ADAMTS-7 deficiency also promoted re-endothelialization and completely blocked subsequent neointima formation. ADAMTS-7 inhibition, therefore,

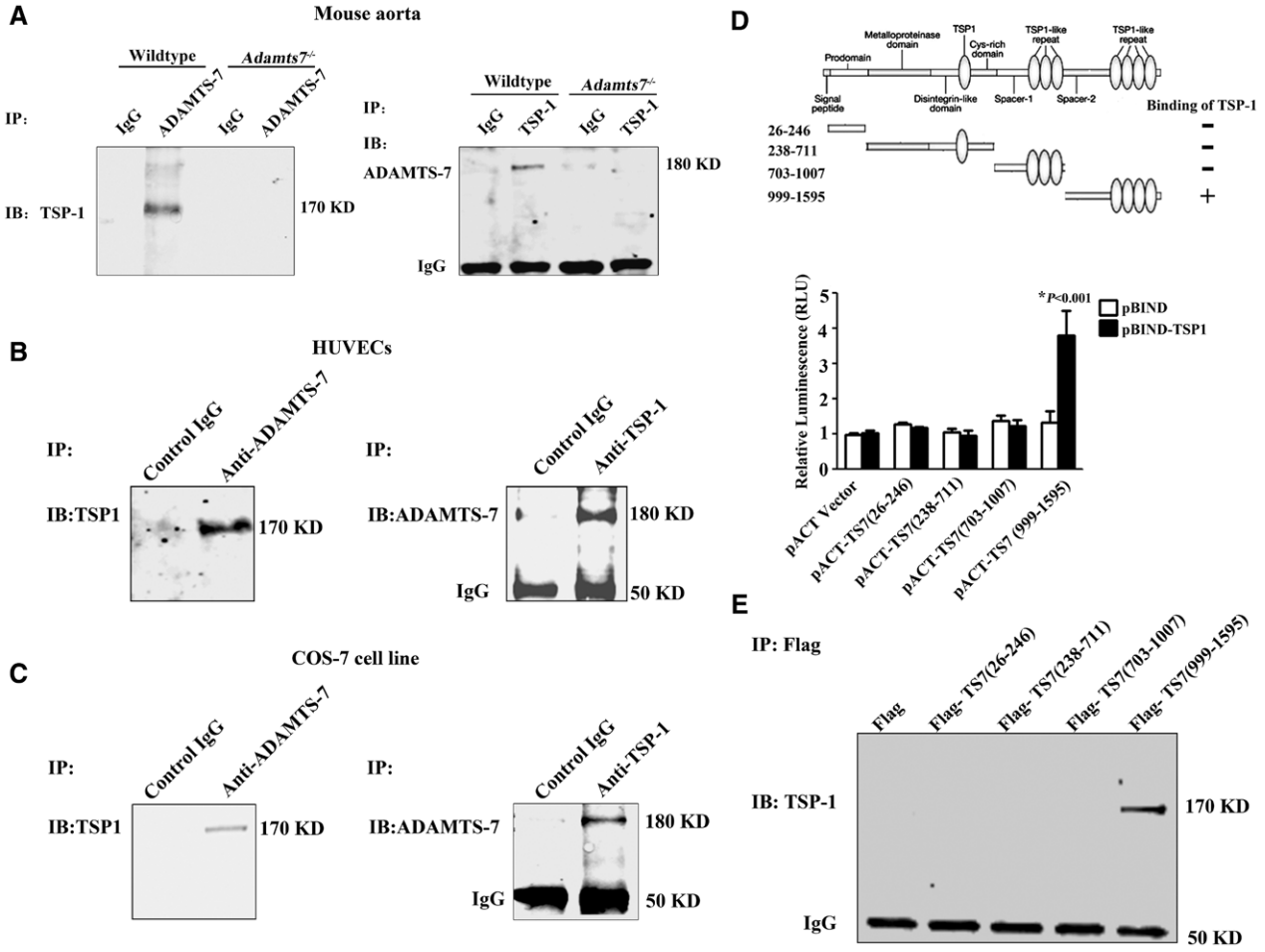

Figure 5. ADAMTS-7 associates with TSP-1 via its C-terminal domain. TSP-1 was associated with ADAMTS-7 in mouse aorta (**A**), HUVECs (**B**) and COS-7 cells cotransfected with TSP-1 and ADAMTS-7 (**C**) by Co-IP. **D**, **Top**, Schematic illustration of ADAMTS-7 structures used to map the corresponding domains that bind to TSP-1. Presence or absence of binding between ADAMTS-7 and TSP-1 was indicated by + or –, respectively. **Bottom**, Mammalian 2-hybrid analysis of ADAMTS-7 and TSP-1 interaction. Eahy 926 cells were cotransfected with pACT plasmids that expressed various ADAMTS-7 deletion mutants and pBIND plasmid that encoded full-length TSP-1. Luciferase activity was analyzed 48 hours after transfection. Data represent the means±SEM of 3 independent experiments in duplicate. **E**, Co-IP of Eahy 926 cells with anti-Flag antibody in vivo. Eahy 926 cells were cotransfected with Flag-CMV vectors that encoded various ADAMTS-7 fragments and full-length TSP-1 for 48 hours. TSP-1 protein expression was examined by Western blot analysis. Co-IP indicates coimmunoprecipitation; HUVEC, human umbilical vein endothelial cell; IB, immunoblot; IgG, immunoglobulin G; IP, immunoprecipitation; SEM, standard error of the mean; and TSP-1, thrombospondin-1.

is a promising dual-effect target for both atherosclerosis and restenosis after PCI.

The *ADAMTS-7* locus was identified to have a strong association with coronary atherosclerotic disease[14,15] and was rather involved in the formation of atherosclerotic plaques in comparison with atherothrombotic events. However, the underlying mechanism is not yet understood. In the current phenotype screening assay, we did not observe difference regarding lipid metabolism. As shown in Table IV in the online-only Data Supplement, without a proatherogenic background, *Adamts7*$^{-/-}$ mice did not display changes in blood lipid levels after 15 weeks of Western diet in comparison with WT mice. However, we did find increased maximum oxygen consumption in male mice (Table II in the online-only Data Supplement), indicating alterations in the energy metabolism or cardiorespiratory fitness during exercise.[24] Further experiments are needed for better understanding of *Adamts7*$^{-/-}$ mice phenotype.

Previously, we demonstrated that ADAMTS-7 degrades COMP in vessels.[10] COMP itself interacts with α7β1 integrin and bone morphogenetic protein 2 and prevents VSMC transdifferentiation into a synthetic or osteogenic phenotype.[11,12] ADAMTS-7, via he degradation of COMP, promotes neointima formation and vascular calcification.[10,17] Among other potential substrates, we have identified TSP-1 as another ADAMTS-7 target with profound functional implications on endothelial biology following injury. ADAMTS-7 not only acts via COMP degradation, but also inhibits EC proliferation/migration via a COMP-independent pathway. TSP-1 belongs to the microcellular thrombospondin protein family, which also includes TSP-2, TSP-3, TSP-4, and TSP-5 (COMP).[25] Our functional data are in line with previous reports that demonstrated that the intra-arterial delivery of TSP-1 antibodies accelerates re-endothelialization and reduces neointimal lesion formation after balloon denudation in rats.[26] Our study is also consistent with earlier studies that showed reduced neointima hyperplasia in *Tsp1*$^{-/-}$ mice.[27] Compelling studies have shown the pivotal role of TSP-1 in angiogenesis, inflammation, wound healing, cancer, and thrombosis via complex protein-protein interactions with various

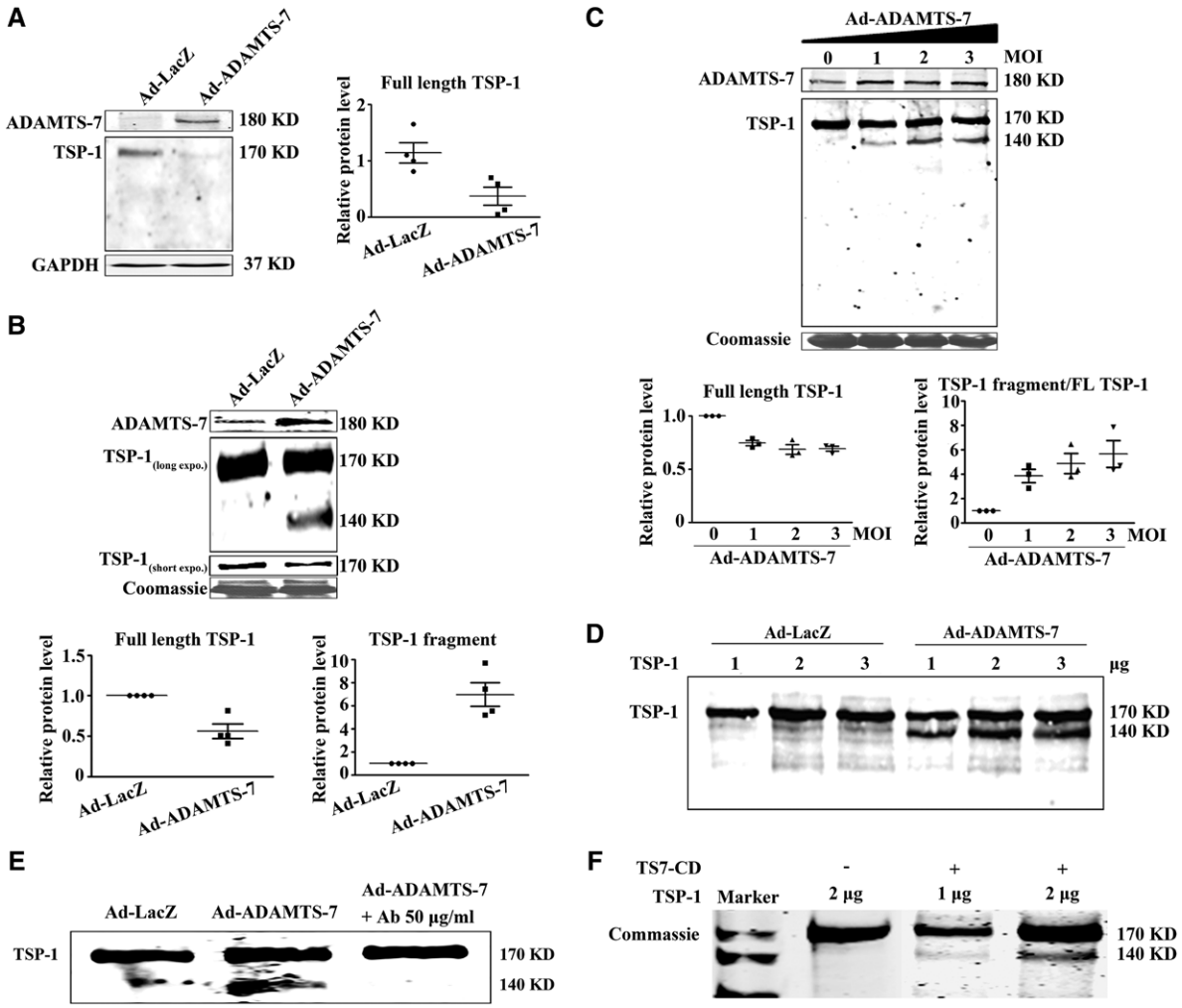

Figure 6. TSP1 is cleaved by ADAMTS-7 in vitro. Western blot of TSP-1 expression in the cell lysate (**A**) and conditional medium (**B**) of HUVECs infected with Ad-*LacZ* and Ad-*ADAMTS-7*, respectively. Results are means±SEM from 4 independent experiments performed. **C** and **D**, Western blots analysis of TSP-1. COS-7 cells were infected with Ad-*ADAMTS-7* or Ad-*LacZ* for 24 hours. Supernatant was concentrated and incubated with hTSP-1 protein for 4 hours in vitro. Data represent the means±SEM of 3 independent experiments. **E**, Representative Western blot of TSP-1. Digestion of hTSP-1 by COS-7 cells infected with Ad-*ADAMTS-7* was abolished by an ADAMTS-7 neutralization antibody (50 μg/mL). n=3. **F**, Catalytic domain of ADAMTS-7 (TS7-CD) digested hTSP-1. Purified hTSP-1 was incubated with the catalytic domain of ADAMTS-7 in vitro. Cleaved products were visualized with Coomassie dye. expo. indicates exposure; FL TSP-1, full-length TSP-1; HUVEC, human umbilical vein endothelial cell; MOI, multiplicity of infection; SEM, standard error of the mean; and TSP-1, thrombospondin-1.

partners, such as CD47, transforming growth factor β, CD36, and integrin.[28] TSP-1 has further been detected in atherosclerotic specimens, and the genetic variants of TSP-1 have been reported to correlate with coronary artery disease and myocardial infarction.[29–31] In *Apoe*$^{-/-}$ mice, TSP-1 deficiency has also been shown to accelerate atherosclerotic plaque maturation without affecting plaque formation.[32] In addition to the inhibition of endothelial recovery, we further ask whether TSP-1 mediates ADAMTS-7 promotion of VSMCs migration. As shown in Figure IV in the online-only Data Supplement, ADAMTS-7 silencing/overexpression–induced repression/enhancement of VSMC migration was not affected by TSP-1 deficiency. In contrast, reduced VSMC migration by ADAMTS-7 silencing was almost completely rescued by COMP deletion, which is in accordance with our previous study,[10] indicating that TSP-1 is not involved in ADAMTS-7–mediated VSMCs migration.

Compelling evidence indicates that TSP-1 was relatively abundant in EC cells or mainly present in endothelium of the stenotic surface of coronary arteries,[29,33] although it was identified in almost all layers of injured arteries. To address the cellular origin of increased TSP-1 in *Adamts7*$^{-/-}$ aorta, we have further isolated the aortic ECs and VSMCs from *Adamts7*$^{-/-}$ and WT mice, respectively. Western blot analysis revealed that TSP-1 protein level increased in both ECs and VSMCs from *Adamts7*$^{-/-}$ mice in comparison with WT mice (Figure V in the online-only Data Supplement). By using enzyme-linked immunosorbent assay analysis, we revealed ≈7-fold basal amount of TSP-1 in the supernatant of EC in comparison with VSMCs (Figure 4A and 4B), indicating that ADAMTS-7 may preferentially target EC TSP-1. However, we cannot exclude the possibility that ADAMTS-7 degrades TSP-1 from both ECs and VSMCs.

Interestingly, both ADAMTS-7 and TSP-1 exhibit potent anti-re-endothelialization effects that cannot simply be explained by reduced expression or secretion of TSP-1 secondary to the cleavage by ADAMTS-7. One potential explanation is that TSP-1 cleavage by enhanced ADAMTS-7 leads

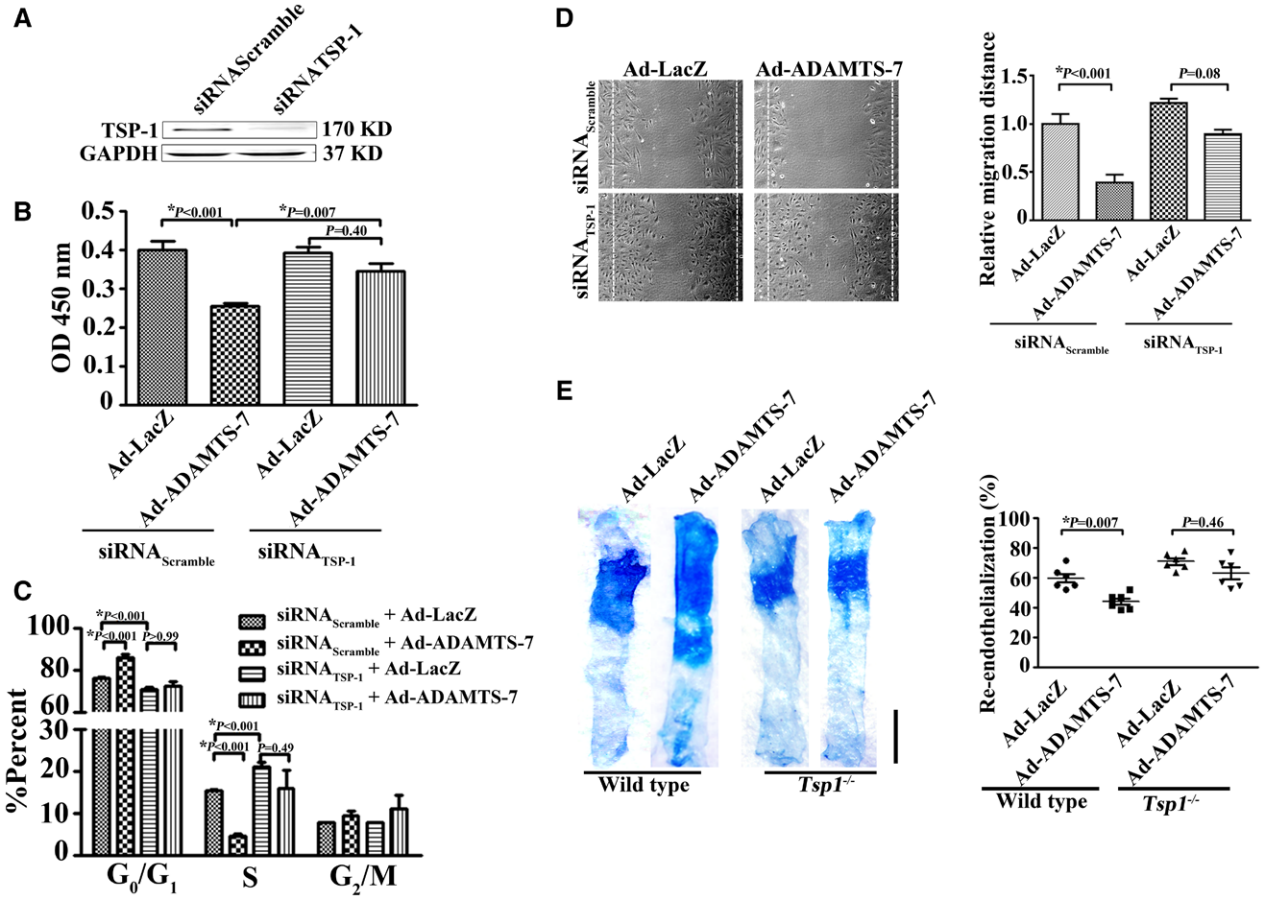

Figure 7. ADAMTS-7 inhibits endothelial cell recovery through the degradation of TSP-1. **A**, Representative Western blots of $siRNA_{scramble}$ and $siRNA_{TSP-1}$ knockdown of TSP-1 protein in HUVECs. **B** and **C**, Silencing of TSP-1 attenuated ADAMTS-7–suppressed HUVEC proliferation. HUVECs were transfected with siRNA 24 hours before adenoviral infection. Twenty-four hours later, the cells were harvested for CCK-8 or FACS analysis. (Results are means±SEM from 3 independent experiments performed in duplicate, **P*<0.05.) **D**, Knockdown of TSP-1 accelerated Ad-*ADAMTS-7*–infected HUVEC migration activity in the wound-scratch assay (magnification ×100; results are means±SEM from 3 independent experiments performed in duplicate, **P*<0.05). **E**, Representative Evans blue staining of en face carotid arteries infected by Ad-*LacZ* or Ad-*ADAMTS-7* 5 days after wire injury in *Tsp1*$^{-/-}$ or wild-type mice (scale bar, 1 mm, re-endothelialization (%) was quantified by Image J, **P*<0.05; n=6 per group). CCK-8 indicates cell counting via kit-8; FACS, fluorescence-activate cell sorting; HUVEC, human umbilical vein endothelial cell; SEM, standard error of the mean; siRNA, small interfering RNA; and TSP-1, thrombospondin-1.

to the production of a bioactive TSP-1 fragment with a more potent inhibitory effect on EC recovery, as demonstrated by a previous study which showed that ADAMTS-1 mediates the release of antiangiogenic polypeptides from TSP-1 and TSP-2.[34] After mutating the ADAMTS-1 cleavage site in TSP-1 (glutamic acid 311 and leonine 312) and cell transfection, the degradation of TSP-1 by ADAMTS-7 was still detectable, which indicates different cleavage sites of ADAMTS-7 and ADAMTS-1, and thus highlights the putative different signaling pathways that involve ADAMTS-7 and TSP-1 (Figure VI in the online-only Data Supplement). Similarly, bioactive extracellular matrix (ECM) fragments generated by matrix metalloproteinases and cathepsins have been shown to exhibit various effects via novel receptors.[35–37] Further studies are needed to clarify the cleavage site of TSP-1 by ADAMTS-7 and the biological function of the cleaved fragment on EC function and vascular repair.

There is other potential possibility of TSP-1–mediated repression of ADAMTS-7 on EC recovery. ADAMTS-7 may release ECM–bound TSP-1 and therefore activate the latent TSP-1. To address this issue, we tried to analyze the ECM-bound TSP-1 in primary *Adamts7*-deficient EC and VSMCs. However, just by regular Western blot analysis we could hardly detect the full-length TSP-1 in the ECM of both ECs and VSMCs (data not shown), whereas abundant TSP-1 was observed in the supernatant. By using a similar protocol, previous studies also found a few ECM-bound TSP-1.[34,38] Previous quantitative proteomics analysis has revealed TSP-1 in the ECM of human vessel, but as a less abundant protein in comparison with other matrix proteins such as fibronectin.[39] Further quantitative ECM proteomics analysis in WT and *Adamts7*$^{-/-}$ aorta is needed to explore the possibility that ADAMTS-7 release of ECM-bound silent TSP-1. Nevertheless, in comparison with the low level of TSP-1 in the ECM, the greater amount of TSP-1 or fragment in the supernatant may play a more important role to EC cells.

In conclusion, ADAMTS-7–mediated TSP-1 cleavage may play an important role in re-endothelialization during human vascular injury-repair response. In addition to its COMP-mediated effects, ADAMTS-7 might involve a second target mechanism for the prevention/therapy of vascular neointima hyperplasia.

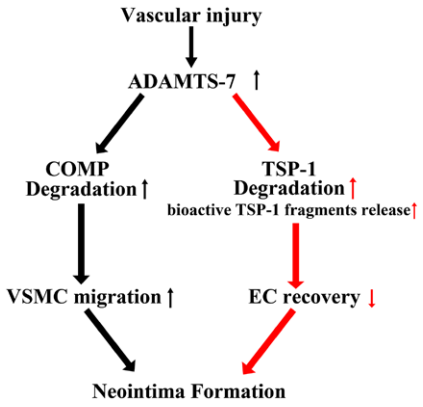

Figure 8. Schematic illustration of ADAMTS-7 on postinjury neointima formation. On one hand, ADAMTS-7 promotes VSMC migration via degradation of COMP, which is pivotal for VSMC homeostasis. On the other hand, ADAMTS-7 degradation of TSP-1 leads to the generation of bioactive TSP-1 fragments that may mediate retarded re-endothelialization and promote neointima formation. COMP indicates cartilage oligomeric matrix protein; EC, endothelial cell; TSP-1, thrombospondin-1; and VSMC, vascular smooth muscle cell.

Acknowledgments

We are grateful for the valuable suggestions of Prof Chuan-ju Liu, New York University School of Medicine. We thank Prof Ake Oldberg from Lund University, Sweden, for kindly providing the *Comp*$^{-/-}$ mice.

Sources of Funding

This research was supported by funding from the International Cooperation and Exchanges NSFC (81220108004); the National Program on Key Basic Research Projects (973 Program; 2012CB518002); the National Natural Science Foundation of the P.R. China (No. 81070243, 81121061, 91339000); the National Science Fund for distinguished Young Scholars (81225002); and the"111" Project of Chinese Ministry of Education (No. B07001). Furthermore, this study was supported by the German Federal Ministry of Education and Research (BMBF) in the context of the e:Med program (*e:AtheroSysMed*), the FP7 European Union project *CVgenes@target* (261123), and by the Foundation Leducq (CADgenomics: Understanding Coronary Artery Disease Genes, 12CVD02). This work was also funded by the German Federal Ministry of Education and Research to the GMC (Infrafrontier grant 01KX1012), to the German Center for Diabetes Research (DZD e.V.), to the German Center for Vertigo and Balance Disorders (grant 01 EO 0901), and by the Initiative and Networking Fund of the Helmholtz Association in the framework of the Helmholtz Alliance for Mental Research in an Ageing Society (HA-215).

Disclosures

None.

References

1. Sitia S, Tomasoni L, Atzeni F, Ambrosio G, Cordiano C, Catapano A, Tramontana S, Perticone F, Naccarato P, Camici P, Picano E, Cortigiani L, Bevilacqua M, Milazzo L, Cusi D, Barlassina C, Sarzi-Puttini P, Turiel M. From endothelial dysfunction to atherosclerosis. *Autoimmun Rev*. 2010;9:830–834. doi: 10.1016/j.autrev.2010.07.016.
2. Versari D, Lerman LO, Lerman A. The importance of reendothelialization after arterial injury. *Curr Pharm Des*. 2007;13:1811–1824.
3. Otsuka F, Nakano M, Ladich E, Kolodgie FD, Virmani R. Pathologic Etiologies of Late and Very Late Stent Thrombosis following First-Generation Drug-Eluting Stent Placement. *Thrombosis*. 2012;2012:608593. doi: 10.1155/2012/608593.
4. Wenaweser P, Daemen J, Zwahlen M, van Domburg R, Jüni P, Vaina S, Hellige G, Tsuchida K, Morger C, Boersma E, Kukreja N, Meier B, Serruys PW, Windecker S. Incidence and correlates of drug-eluting stent thrombosis in routine clinical practice. 4-year results from a large 2-institutional cohort study. *J Am Coll Cardiol*. 2008;52:1134–1140. doi: 10.1016/j.jacc.2008.07.006.
5. Maeng M, Tilsted HH, Jensen LO, Kaltoft A, Kelbæk H, Abildgaard U, Villadsen AB, Krusell LR, Ravkilde J, Hansen KN, Christiansen EH, Aarøe J, Jensen JS, Kristensen SD, Bøtker HE, Madsen M, Thayssen P, Sørensen HT, Thuesen L, Lassen JF. 3-Year clinical outcomes in the randomized SORT OUT III superiority trial comparing zotarolimus- and sirolimus-eluting coronary stents. *JACC Cardiovasc Interv*. 2012;5:812–818. doi: 10.1016/j.jcin.2012.04.008.
6. Joner M, Finn AV, Farb A, Mont EK, Kolodgie FD, Ladich E, Kutys R, Skorija K, Gold HK, Virmani R. Pathology of drug-eluting stents in humans: delayed healing and late thrombotic risk. *J Am Coll Cardiol*. 2006;48:193–202. doi: 10.1016/j.jacc.2006.03.042.
7. Finn AV, Joner M, Nakazawa G, Kolodgie F, Newell J, John MC, Gold HK, Virmani R. Pathological correlates of late drug-eluting stent thrombosis: strut coverage as a marker of endothelialization. *Circulation*. 2007;115:2435–2441. doi: 10.1161/CIRCULATIONAHA.107.693739.
8. Newby AC. Matrix metalloproteinases regulate migration, proliferation, and death of vascular smooth muscle cells by degrading matrix and non-matrix substrates. *Cardiovasc Res*. 2006;69:614–624. doi: 10.1016/j.cardiores.2005.08.002.
9. Liu CJ, Kong W, Ilalov K, Yu S, Xu K, Prazak L, Fajardo M, Sehgal B, Di Cesare PE. ADAMTS-7: a metalloproteinase that directly binds to and degrades cartilage oligomeric matrix protein. *FASEB J*. 2006;20:988–990. doi: 10.1096/fj.05-3877fje.
10. Wang L, Zheng J, Bai X, Liu B, Liu CJ, Xu Q, Zhu Y, Wang N, Kong W, Wang X. ADAMTS-7 mediates vascular smooth muscle cell migration and neointima formation in balloon-injured rat arteries. *Circ Res*. 2009;104:688–698. doi: 10.1161/CIRCRESAHA.108.188425.
11. Wang L, Zheng J, Du Y, Huang Y, Li J, Liu B, Liu CJ, Zhu Y, Gao Y, Xu Q, Kong W, Wang X. Cartilage oligomeric matrix protein maintains the contractile phenotype of vascular smooth muscle cells by interacting with alpha(7)beta(1) integrin. *Circ Res*. 2010;106:514–525. doi: 10.1161/CIRCRESAHA.109.202762.
12. Du Y, Wang Y, Wang L, Liu B, Tian Q, Liu CJ, Zhang T, Xu Q, Zhu Y, Ake O, Qi Y, Tang C, Kong W, Wang X. Cartilage oligomeric matrix protein inhibits vascular smooth muscle calcification by interacting with bone morphogenetic protein-2. *Circ Res*. 2011;108:917–928. doi: 10.1161/CIRCRESAHA.110.234328.
13. Schunkert H, König IR, Kathiresan S, Reilly MP, Assimes TL, Holm H, Preuss M, Stewart AF, Barbalic M, Gieger C, Absher D, Aherrahrou Z, Allayee H, Altshuler D, Anand SS, Andersen K, Anderson JL, Ardissino D, Ball SG, Balmforth AJ, Barnes TA, Becker DM, Becker LC, Berger K, Bis JC, Boekholdt SM, Boerwinkle E, Braund PS, Brown MJ, Burnett MS, Buysschaert I, Carlquist JF, Chen L, Cichon S, Codd V, Davies RW, Dedoussis G, Dehghan A, Demissie S, Devaney JM, Diemert P, Do R, Doering A, Eifert S, Mokhtari NE, Ellis SG, Elosua R, Engert JC, Epstein SE, de Faire U, Fischer M, Folsom AR, Freyer J, Gigante B, Girelli D, Gretarsdottir S, Gudnason V, Gulcher JR, Halperin E, Hammond N, Hazen SL, Hofman A, Horne BD, Illig T, Iribarren C, Jones GT, Jukema JW, Kaiser MA, Kaplan LM, Kastelein JJ, Khaw KT, Knowles JW, Kolovou G, Kong A, Laaksonen R, Lambrechts D, Leander K, Lettre G, Li M, Lieb W, Loley C, Lotery AJ, Mannucci PM, Maouche S, Martinelli N, McKeown PP, Meisinger C, Meitinger T, Melander O, Merlini PA, Mooser V, Morgan T, Mühleisen TW, Muhlestein JB, Münzel T, Musunuru K, Nahrstaedt J, Nelson CP, Nöthen MM, Olivieri O, Patel RS, Patterson CC, Peters A, Peyvandi F, Qu L, Quyyumi AA, Rader DJ, Rallidis LS, Rice C, Rosendaal FR, Rubin D, Salomaa V, Sampietro ML, Sandhu MS, Schadt E, Schäfer A, Schillert A, Schreiber S, Schrezenmeir J, Schwartz SM, Siscovick DS, Sivananthan M, Sivapalaratnam S, Smith A, Smith TB, Snoep JD, Soranzo N, Spertus JA, Stark K, Stirrups K, Stoll M, Tang WH, Tennstedt S, Thorgeirsson G, Thorleifsson G, Tomaszewski M, Uitterlinden AG, van Rij AM, Voight BF, Wareham NJ, Wells GA, Wichmann HE, Wild PS, Willenborg C, Witteman JC, Wright BJ, Ye S, Zeller T, Ziegler A, Cambien F, Goodall AH, Cupples LA, Quertermous T, März W, Hengstenberg C, Blankenberg S, Ouwehand WH, Hall AS, Deloukas P, Thompson JR, Stefansson K, Roberts R, Thorsteinsdottir U, O'Donnell CJ, McPherson R, Erdmann J, Samani NJ; Cardiogenics; CARDIoGRAM Consortium. Large-scale association analysis identifies 13 new susceptibility loci for coronary artery disease. *Nat Genet*. 2011;43:333–338. doi: 10.1038/ng.784.

14. Reilly MP, Li M, He J, Ferguson JF, Stylianou IM, Mehta NN, Burnett MS, Devaney JM, Knouff CW, Thompson JR, Horne BD, Stewart AF, Assimes TL, Wild PS, Allayee H, Nitschke PL, Patel RS, Martinelli N, Girelli D, Quyyumi AA, Anderson JL, Erdmann J, Hall AS, Schunkert H, Quertermous T, Blankenberg S, Hazen SL, Roberts R, Kathiresan S, Samani NJ, Epstein SE, Rader DJ; Myocardial Infarction Genetics Consortium; Wellcome Trust Case Control Consortium. Identification of ADAMTS7 as a novel locus for coronary atherosclerosis and association of ABO with myocardial infarction in the presence of coronary atherosclerosis: two genome-wide association studies. *Lancet*. 2011;377:383–392. doi: 10.1016/S0140-6736(10)61996-4.
15. Consortium CADCDG. A genome-wide association study in Europeans and South Asians identifies five new loci for coronary artery disease. *Nat Genet*. 2011;43:339–344.
16. Pu X, Xiao Q, Kiechl S, Chan K, Ng FL, Gor S, Poston RN, Fang C, Patel A, Senver EC, Shaw-Hawkins S, Willeit J, Liu C, Zhu J, Tucker AT, Xu Q, Caulfield MJ, Ye S. ADAMTS7 cleavage and vascular smooth muscle cell migration is affected by a coronary-artery-disease-associated variant. *Am J Hum Genet*. 2013;92:366–374. doi: 10.1016/j.ajhg.2013.01.012.
17. Du Y, Gao C, Liu Z, Wang L, Liu B, He F, Zhang T, Wang Y, Wang X, Xu M, Luo GZ, Zhu Y, Xu Q, Wang X, Kong W. Upregulation of a disintegrin and metalloproteinase with thrombospondin motifs-7 by miR-29 repression mediates vascular smooth muscle calcification. *Arterioscler Thromb Vasc Biol*. 2012;32:2580–2588. doi: 10.1161/ATVBAHA.112.300206.
18. Lindner V, Fingerle J, Reidy MA. Mouse model of arterial injury. *Circ Res*. 1993;73:792–796.
19. Yin X, Bern M, Xing Q, Ho J, Viner R, Mayr M. Glycoproteomic analysis of the secretome of human endothelial cells. *Mol Cell Proteomics*. 2013;12:956–978. doi: 10.1074/mcp.M112.024018.

19a. University of California Davis and Children's Hospital Oakland Research Institute. Trans-NIH Knock-Out Mouse Project, KOMP Repository, USA. http://www.komp.org. Accessed March 17, 2015.

20. Gailus-Durner V, Fuchs H, Becker L, Bolle I, Brielmeier M, Calzada-Wack J, Elvert R, Ehrhardt N, Dalke C, Franz TJ, Grundner-Culemann E, Hammelbacher S, Hölter SM, Hölzlwimmer G, Horsch M, Javaheri A, Kalaydjiev SV, Klempt M, Kling E, Kunder S, Lengger C, Lisse T, Mijalski T, Naton B, Pedersen V, Prehn C, Przemeck G, Racz I, Reinhard C, Reitmeir P, Schneider I, Schrewe A, Steinkamp R, Zybill C, Adamski J, Beckers J, Behrendt H, Favor J, Graw J, Heldmaier G, Höfler H, Ivandic B, Katus H, Kirchhof P, Klingenspor M, Klopstock T, Lengeling A, Müller W, Ohl F, Ollert M, Quintanilla-Martinez L, Schmidt J, Schulz H, Wolf E, Wurst W, Zimmer A, Busch DH, de Angelis MH. Introducing the German Mouse Clinic: open access platform for standardized phenotyping. *Nat Methods*. 2005;2:403–404. doi: 10.1038/nmeth0605-403.
21. Riessen R, Fenchel M, Chen H, Axel DI, Karsch KR, Lawler J. Cartilage oligomeric matrix protein (thrombospondin-5) is expressed by human vascular smooth muscle cells. *Arterioscler Thromb Vasc Biol*. 2001;21:47–54.
22. Tuszynski GP, Nicosia RF. The role of thrombospondin-1 in tumor progression and angiogenesis. *Bioessays*. 1996;18:71–76. doi: 10.1002/bies.950180113.
23. DiPietro LA, Nebgen DR, Polverini PJ. Downregulation of endothelial cell thrombospondin 1 enhances *in vitro* angiogenesis. *J Vasc Res*. 1994;31:178–185.
24. Bassett DR Jr, Howley ET. Limiting factors for maximum oxygen uptake and determinants of endurance performance. *Med Sci Sports Exerc*. 2000;32:70–84.
25. Good DJ, Polverini PJ, Rastinejad F, Le Beau MM, Lemons RS, Frazier WA, Bouck NP. A tumor suppressor-dependent inhibitor of angiogenesis is immunologically and functionally indistinguishable from a fragment of thrombospondin. *Proc Natl Acad Sci U S A*. 1990;87:6624–6628.
26. Chen D, Asahara T, Krasinski K, Witzenbichler B, Yang J, Magner M, Kearney M, Frazier WA, Isner JM, Andrés V. Antibody blockade of thrombospondin accelerates reendothelialization and reduces neointima formation in balloon-injured rat carotid artery. *Circulation*. 1999;100:849–854.
27. Moura R, Tjwa M, Vandervoort P, Cludts K, Hoylaerts MF. Thrombospondin-1 activates medial smooth muscle cells and triggers neointima formation upon mouse carotid artery ligation. *Arterioscler Thromb Vasc Biol*. 2007;27:2163–2169. doi: 10.1161/ATVBAHA.107.151282.
28. Lawler PR, Lawler J. Molecular basis for the regulation of angiogenesis by thrombospondin-1 and -2. *Cold Spring Harb Perspect Med*. 2012;2:a006627. doi: 10.1101/cshperspect.a006627.
29. Reed MJ, Iruela-Arispe L, O'Brien ER, Truong T, LaBell T, Bornstein P, Sage EH. Expression of thrombospondins by endothelial cells. Injury is correlated with TSP-1. *Am J Pathol*. 1995;147:1068–1080.
30. Ashokkumar M, Anbarasan C, Saibabu R, Kuram S, Raman SC, Cherian KM. An association study of thrombospondin 1 and 2 SNPs with coronary artery disease and myocardial infarction among South Indians. *Thromb Res*. 2011;128:e49–e53. doi: 10.1016/j.thromres.2011.05.026.
31. Riessen R, Kearney M, Lawler J, Isner JM. Immunolocalization of thrombospondin-1 in human atherosclerotic and restenotic arteries. *Am Heart J*. 1998;135(2 Pt 1):357–364.
32. Moura R, Tjwa M, Vandervoort P, Van Kerckhoven S, Holvoet P, Hoylaerts MF. Thrombospondin-1 deficiency accelerates atherosclerotic plaque maturation in ApoE-/- mice. *Circ Res*. 2008;103:1181–1189. doi: 10.1161/CIRCRESAHA.108.185645.
33. Mosher DF, Doyle MJ, Jaffe EA. Synthesis and secretion of thrombospondin by cultured human endothelial cells. *J Cell Biol*. 1982;93:343–348.
34. Lee NV, Sato M, Annis DS, Loo JA, Wu L, Mosher DF, Iruela-Arispe ML. ADAMTS1 mediates the release of antiangiogenic polypeptides from TSP1 and 2. *EMBO J*. 2006;25:5270–5283. doi: 10.1038/sj.emboj.7601400.
35. Sage H. Pieces of eight: bioactive fragments of extracellular proteins as regulators of angiogenesis. *Trends Cell Biol*. 1997;7:182–186.
36. Petitclerc E, Boutaud A, Prestayko A, Xu J, Sado Y, Ninomiya Y, Sarras MP Jr, Hudson BG, Brooks PC. New functions for non-collagenous domains of human collagen type IV. Novel integrin ligands inhibiting angiogenesis and tumor growth in vivo. *J Biol Chem*. 2000;275:8051–8061.
37. Hamano Y, Zeisberg M, Sugimoto H, Lively JC, Maeshima Y, Yang C, Hynes RO, Werb Z, Sudhakar A, Kalluri R. Physiological levels of tumstatin, a fragment of collagen IV alpha3 chain, are generated by MMP-9 proteolysis and suppress angiogenesis via alphaV beta3 integrin. *Cancer Cell*. 2003;3:589–601.
38. Bonnefoy A, Legrand C. Proteolysis of subendothelial adhesive glycoproteins (fibronectin, thrombospondin, and von Willebrand factor) by plasmin, leukocyte cathepsin G, and elastase. *Thromb Res*. 2000;98:323–332.
39. Didangelos A, Yin X, Mandal K, Baumert M, Jahangiri M, Mayr M. Proteomics characterization of extracellular space components in the human aorta. *Mol Cell Proteomics*. 2010;9:2048–2062. doi: 10.1074/mcp.M110.001693.

CLINICAL PERSPECTIVE

Besides vascular smooth muscle cell proliferation and migration, the rate of luminal endothelial recovery is also a critical modulator of neointima formation after vascular injury. Here, we show that ADAMTS-7 may affect both processes. ADAMTS-7, a member of the disintegrin and metalloproteinase with thrombospondin motifs (ADAMTS) family, was recently identified to be genomewide significantly associated with human coronary artery disease. We have previously shown that ADAMTS-7 can promote vascular smooth muscle cell migration and neointima formation after artery injury via the degradation of cartilage oligomeric matrix protein. In this study, we show that *Adamts7*$^{-/-}$ mice exhibited greater re-endothelialization and were completely resistant to neointima formation on injury. ADAMTS-7 inhibition may serve as new strategy to promote endothelial recovery, and, simultaneously, to inhibit vascular smooth muscle cells activation for the effective prevention and treatment of atherosclerosis and postinjury restenosis. Furthermore, the identification of thrombospondin-1 as an ADAMTS-7 target on one hand, and as a modulator of vascular remodeling on the other, might lead to the elucidation of further druggable downstream targets.

SUPPLEMENTAL MATERIAL.

Supplemental Methods

Materials

Antibody against ADAMTS-7 was purchased from Abcam (Cambridge, UK). Antibodies against Thrombospondin-1 (TSP-1) were purchased from Neomarkers (Fremont, CA). Antibodies against BrdU were purchased from Sigma-Aldrich (St. Louis, MO). The antibody against GAPDH was purchased from Cell Signaling Technology (Boston, MA). The antibody against vWF was purchased from Santa Cruz Biotechnology (Santa Cruz, CA). The antibodies against Cyclin D1 and E1 were purchased from Bioworld (Minneapolis, MN). The neutralizing antibody of ADAMTS-7 (Antigen: LEDEEKDLKITH-KLH) was purchased from Biosynthesis Biotechnology Co., Ltd. (Beijing, China). Recombinant human TSP-1 was purchased from R&D Systems (Minneapolis, MN).

Generation of *Adamts7*$^{-/-}$ mice

The *Adamts7* knockout embryonic stem cell (*Adamts7*-KO-ESC) line (EPD0209) was purchased from the European Conditional Mouse Mutagenesis Program (EUCOMM)[1]. Microinjection of *Adamts7*-KO-ESC into C57BL/6N blastocysts was achieved at the Knock Out Mouse Project (KOMP) repository at the University of California, Davis, USA[2]. The *Adamts7* targeting vector includes the insertion of a neomycin selection cassette and two loxP sites flanking exon 5 and exon 6 in the *Adamts7* genomic sequence. The *Adamts7* gene was interrupted by introducing an internal ribosome entry site followed by the beta-galactosidase sequence between exons 4 and 5. Male chimeras were obtained and backcrossed to C57BL/6

females in our animal facility to generate founders, which were then selected and genotyped using polymerase chain reaction (PCR) on genomic DNA isolated from ear punch biopsies. Heterozygous mice were intercrossed to generate knockout (*Adamts7*$^{-/-}$), heterozygous (*Adamts7*$^{+/-}$) and wildtype (WT) littermates. Genomic DNA was isolated from ear punches using standard methods. Tissue sections from mice were explanted, snap-frozen in liquid nitrogen and stored at -80°C until use. Homogenization and RNA-isolation were performed using TRIzol (Life Technologies) according to the manufacturer's recommendations. RNA was stored at -80°C until use. cDNA was generated using M-MLV Reverse Transcriptase (Life Technologies) and pdN6-Primers. Amplification of DNA and cDNA was performed using rTaq (GE Healthcare) with the recommended supplements. PCR-products were visualized on agarose-gels.

X-gal staining of cryosections

Organs were excised and embedded in Tissue Tek (Sakura), snap frozen in liquid nitrogen, and stored at -20°C until use. The tissues were sectioned into 8-10 µm cryosections. For X-gal staining, the cryosections were air dried, incubated in PBS that contained 0.5% glutaraldehyde at 4°C for 10 min, washed in PBS and incubated with X-gal (5-bromo-4-chloro-3-indolyl-β-D-galactopyranoside) solution at 37°C overnight. Afterwards, the cryosections were washed in PBS, dehydrated and mounted using cover slips (Fisher).

Large-Scale phenotyping of *Adamts7*$^{-/-}$ mice

All animal studies followed the guidelines of the Animal Care and Use Committees of

Peking University, People's Republic of China, Schleswig-Holstein and Bavaria, Germany. Fifty-four mice, i.e., 29 females (15 WT, 14 *Adamts7*$^{-/-}$) and 25 males (10 WT, 15 *Adamts7*$^{-/-}$), were generated by intercrossing heterozygous *Adamts7*$^{+/-}$-mice and transferred to the German Mouse Clinic (GMC). At the GMC mice were maintained in IVC cages (Ventirack, Biozone, UK) with water and standard mouse chow (Altromin no. 1324) according to the GMC housing conditions and German laws.The mice were processed by standardized screening procedures as described previously[3, 4]. Briefly, the mice were characterized regarding morphology, behavior, neurology, eye morphology and function, nociception, energy metabolism, clinical chemistry/ hematology, immunology, allergies, steroid metabolism, cardiovascular function, lung function, and pathology.

Wire-injury of mouse carotid artery

Wire-injury of the mouse carotid artery was performed in 12-week-old mice as described by Lindner et al[5]. Through a middle line neck incision on the ventral side, the left common carotid artery (LCCA), including bifurcation, was exposed and cleaned from the surrounding tissue. Bulldog clamps were placed around the LCCA proximal to the aortic arch and the left internal carotid artery (LICA) for temporary control of blood flow; a 6-0 suture was placed around the left external carotid artery (LECA). An incision hole was made in the LECA, then a flexible wire (0.38 mm) was introduced into the LCCA by approximately 5 mm and passed 3 times toward and forth with rotation. The wire was removed, and the LECA was then tied off proximally. The skin incision was closed with surgical sutures. The area of remaining denudation at 3, 5 and 7 days after injury was determined by left ventricle injection of Evans

blue dye; quantification of the dye-stained area by blinded image analysis was performed as described previously[6]. Fourteen and 28 days after injury, the mouse arteries were harvested and embedded in Tissue Tek OCT (Sakura Finetek, Staufen, Germany); 6 μm serial cryostat sections were obtained from the bifurcation point and analyzed by matoxylin/eosin staining and Spot Image software (Diagnostic Instruments, Australia). All surgical studies followed the guidelines of the Animal Care and Use Committee of Peking University.

BrdU incorporation

BrdU incorporation was performed 3 days after injury as described previously[7]. Briefly, BrdU was administered to mice via an intraperitoneal injection at 48, 24, and 2 hours prior to sacrifice. The carotid arteries were then harvested and incubated with anti-BrdU and anti-vWF antibodies to perform dual immunofluorescence staining.

Femoral artery injury in mice

Thrombospondin-1 deficient (*Tsp1*$^{-/-}$) mice were purchased from Jackson Lab. A wire-mediated vascular injury was induced in the femoral arteries of *Tsp1*$^{-/-}$ or WT mice by an angioplasty guide wire as described previously[8]. Briefly, the femoral arteries were exposed by a longitudinal groin incision and monitored under a surgical microscope. The femoral artery was temporarily clamped at the level of the inguinal ligament, and an incision hole was created distal to the deep femoral branch. After release of the clamp, a 0.38-mm guide wire was advanced once by approximately 5 mm and was left in place for 1 minute to denude and dilate the artery. The wire was then removed, and the arteriotomy site was ligated with an 8-0

suture. For *in vivo* overexpression, a single exposure of 5×10^8 plaque forming units (pfus) of Ad-ADAMTS7 or Ad-LacZ adenovirus were delivered to the wire-injured femoral artery segments. The skin incision was closed with a 6-0 silk suture. The animals were monitored as per usual after surgery. ADAMTS-7 overexpression *in vivo* was confirmed by immunohistochemistry 3 days after adenovirus delivery (data not shown). Re-endothelialization of the femoral artery was determined by Evans blue staining 5 days after wire injury in mice.

Immunohistochemistry and Dual Immunofluorescence

To confirm ADAMTS-7 overexpression in femoral arteries, frozen sections of carotid arteries were incubated with rabbit primary anti-ADAMTS-7 antibody (Abcam, Cambridge, UK), horseradish peroxidase-conjugated goat anti-rabbit IgG and 3, 3-diaminobenzidine, successively. The sections were then counterstained with hematoxylin. For dual immunofluorescence, the frozen sections were first incubated with the antibodies mouse anti-BrdU (1:200) and rabbit anti-vWF (1:50) and then the secondary TRITC-conjugated goat anti-rabbit IgG (1:300) and FITC-conjugated goat anti-mouse IgG (1:300) (Rockland Inc. Gilbertsville, PA), respectively. Fluorescence was detected by confocal laser scanning microscopy (Leica, Germany).

Cell culture

HUVECs were isolated from human umbilical veins by type I collagenase (100 IU/ml) and by the differential attachment rate from other cells[9]. Human umbilical cords were

obtained from Peking University Third Hospital. The experiment was approved by the Ethics Committee of the Peking University Health Science Center, and it was conducted after informed consent was provided by the infants' parents. Cells were cultured in medium 199 (Gibco) that contained 10% fetal bovine serum (FBS, Hyclone), 4.17 mg/L recombinant human endothelial cell growth factor (Sigma), 1.4 IU/ml heparin sodium (Sigma), 3.0 mg/L thymidine (Sigma), 5.96 g/L HEPES, 2.2 g/L $NaHCO_3$, 200 U/mL penicillin, and 100 U /mL streptomycin and passaged by 0.05% trypsin digestion. HUVECs of passage 5–6 were used for experiments.

Real-Time Quantitative PCR and Western Blot Analysis

Real-time PCR amplification involved the use of an Mx3000 Multiplex Quantitative PCR System (Stratagene Corp, La Jolla, CA) and SYBR Green I reagent normalized to that of the internal control β-actin. The specific primers for human ADAMTS-7 were sense, 5’-GTGGAGACCCTGGTAGTAGC-3’, and antisense, 5’-TCTGCGTGGTGCGTGATCTTTA-3’. The primers for human Thrombospondin-1 were sense, 5’-GACTCCTAGAACGTGCGACCT-3’, and antisense, 5’-CATACAATCGTCTCGGGTATGC-3’, and the primers for human β -actin were sense, 5’-ATCTGGCACCACACCTTC-3’, and antisense, 5’-AGCCAGGTCCAGACGCA-3’. All amplification reactions were conducted over 40 cycles (an initial stage of 7 min at 94°C, then a three-step program of 30 s at 94°C, 30 s at 58°C and 30 s at 72°C) and were performed in duplicate.

Extracts that contained equal amounts of total protein were resolved by 10% or 6-20%

gradient SDS-PAGE. The membranes were incubated with primary antibody and IRDye 700DX-conjugated secondary antibodies (Rockland Inc., Gilbertsville, Pa). The immunofluorescence signal was detected by the Odyssey infrared imaging system (LI-COR Biosciences, Lincoln, NE).

Cell proliferation assay

After infected with Ad-LacZ or ADAMTS-7 for 48h, HUVECs were trypsinized to single-cell suspension, and 3000 cells in M199 that contained 10% FBS were transferred to each well of a 96-well plate. Cell Counting Kit-8(CCK-8) reagent was added 24 hours after synchronization and incubated at 37°C for 2 to 4 hours according to the color change. The OD (optical density) value at 450 nm was read by a microplate reader (Varioskan Flash, Thermo Fisher). For cell cycle analyses, HUVECs were fixed with 70% ethanol and then stained with 20 μg/mL propidium iodide (PI) and 500 mg/mL RNase A (Sigma), followed by FACS analysis. Each experiment was performed a minimum of 3 times independently.

Cell migration assay

HUVECs were infected with Ad-LacZ or ADAMTS-7 for 48h before sratching assay and the modified Boyden Chamber analysis. For the scratching assay, HUVECs (3×10^5 cells) were seeded in 6-well plates. The medium was changed to serum-free OPTI-MEM for synchronization after adenoviral infection. Six hours later, scratching was made, and fresh medium that contained 10% FBS was added. Four fields were randomly selected in each well

to record gap distances immediately following scratching at 12, 18 and 24 hours to calculate cell migration.

A modified Boyden Chamber (Chemicon International, MA) coated with an 8-μm barrier of collagen type I was used to test the HUVECs migration ability. For this, 200 μl of suspended HUVECs (2×10^5/ml in M199 that contained 10% FBS) were placed in the upper chamber. The lower chamber contained PDGF-BB (20 ng/ml) as a chemoattractant. After 6, 9 or 12 hours, cells on the upper surface were removed by gentle abrasion with the use of a cotton bud, and cells on the underside (invaded cells) were fixed and stained with crystal violet. The mean number of cells on the lower surface was counted from 4 randomly chosen high-power fields (×100) under light microscopy in 3 independent experiments.

Gel-LC-MS analysis of secretome

Analysis of the secretome was performed as described[10]. Rat VSMCs were infected with adenovirus that contained GFP or ADAMTS-7. Conditioned media were precipitated with acetone and denatured with 2× SDS sample buffer (Invitrogen) at 97°C for 5 min. Proteins were separated on 4%-12% NuPAGE Bis-Tris gels (Invitrogen). After silver staining, each lane was cut into 16 gel bands without gaps and digested with trypsin (Promega) using a robotic digestor (ProGest, Digilab) overnight. Peptides were separated by nano-flow HPLC on a reverse-phase column (C18 PepMap 100, 3 μm, 100 Å, 25 cm; Thermo Fisher Scientific) and identified by a LTQ Orbitrap XL mass spectrometer (Thermo Fisher Scientific). Spectra were acquired with the full MS scan range of m/z 450-2000 followed by six dependent MS2

scans using dynamic exclusion. The results were blasted against the UniProt/SwissProt database (SwissProt 57.15, 515203 entries) using Mascot server 2.3.01 (Matrix Science). The following parameters were used: peptide tolerance = 10 ppm, fragment tolerance = 0.8 Da, carbamidomethylation of cysteine as fixed modification, oxidation of methionine as variable modification, and 2 missed cleavages were allowed. Scaffold (version 3.6.2, Proteome Software) was used to validate MS/MS-based peptide and protein identification with the following filters: peptide probability > 95%, protein probability > 99%, and minimum no. peptides per protein ≥ 2.

Co-Immunoprecipitation

Cells or rat aorta artery lysates were incubated with anti-ADAMTS-7 or anti-TSP-1 antibodies prior to immunoprecipitation with protein P/A agarose beads (Santa Cruz, CA). The precipitated proteins were resolved by 10% SDS-PAGE and immunoblotted with anti-TSP-1 or anti-ADAMTS-7 antibodies, respectively. Rabbit or mouse IgG antibodies served as a negative control.

In another site of study, Eahy 926 cells were co-transfected with Flag-CMV vectors that encoded various ADAMTS-7 fragments (Flag-TS7(26-246), Flag-TS7(238-711), Flag-TS7(703-1007), and Flag-TS7(999-1595) and full length TSP-1 for 48 hours respectively. Cell lysates were incubated with anti-Flag antibody and then immunoblotted with anti-TSP-1 antibodies.

TSP1 siRNA Transfection

Small interfering RNA (siRNA) against human TSP-1 was purchased from GenePharma Co., Ltd (Shanghai). Sequences corresponding to the siRNA of TSP-1 were sense, 5'-GCGUGUUUGACAUCUUUGATT-3', and antisense, 5'-UCAAAGAUGUCAAACACGCTT-3'. Transfection of HUVECs with siRNA (20 nmol/L) *in vitro* was performed using RNAi MAX (Invitrogen). A scramble stealth RNAi duplex served as a negative control.

Subcloning TSP-1 plasmid

The cDNA fragment encoding the full-length human *TSP1* (NCBI Reference sequence: NM_003246.2) was cloned into the *SalI/XbaI* sites of pDNR-CMV and pFlag-CMV plasmid. The primer sequences were sense, 5'-TGCTCTAGAACAGGATCCCTGCTGGGCACCAACA-3', and antisense, 5'-CGGGGTACCTCCAGAAGGTGCAATACCAGCATTGG-3'.

Mammalian two-hybrid assay

The fragments that encoded the 4 functional domains of rat *ADAMTS-7* (i.e., the prodomain [TS7(26-246); aa 26-246], the metalloproteinase plus disintegrin-like and cysteine-rich domain [TS7(238-711); aa 238-711], the spacer-1 plus three TSP repeats [TS7(703-1007); aa 703-1007], and the spacer-2 plus four C-terminal TSP repeats [TS7(999-1595); aa 999-1595]) were amplified by PCR and subcloned in-frame into the *Sal*I/*Xba*I or *Ecor*V/*Xba*I sites of pACT (pACT-TS7(26-246), pACT-TS7(238-711), pACT-TS7(703-1007), and pACT-TS7(999-1595), respectively. cDNA inserts that encoded

human TSP-1 were subcloned in-frame into the pBIND vector to generate the indicated plasmids (pBIND-TSP-1). Eahy 926 cells were cotransfected with the target and bait constructs, together with the reporter plasmid pG5luc-luciferase at a ratio of 1:1:1. After 48 h, the transfected cells were harvested, and the cell lysates were used for a luciferase assay with the Dual-Luciferase Reporter Assay System (Promega). The fragment primer sequences are listed in Supplemental Table 6.

Mutagenesis of TSP-1

The ADAMTS-1 cleavage site in TSP-1 (glutamic acid 311 and leonine 312)[11] were mutated to Isoleucine and Asparagine respectively. Site-mutation was mediated by DpnI-Restriktionsendonuklease (Takara).

***In vitro* digestion of TSP1**

The digestion assay was performed as described previously[11]. Briefly, COS-7 cells were infected with adenovirus that expressed LacZ (control) or ADAMTS-7 for 48 hours. The medium was then changed to serum-free DMEM. The culture medium (CM) was collected after 24 h of incubation and concentrated by centrifugal filter devices (Amicon Ultra-0.5, Millipore). Purified hTSP-1 (R&D) was incubated with CM from adenoviral infected cells at 37°C for 4 hours.

Cleavage of TSP-1 by recombinant catalytic domain of ADAMTS-7 *in vitro*

The bacterial expression vector pGEX-6p-1 was used to produce recombinant

glutathione S-transferase (GST) fusion proteins in *Escherichia coli*. The cDNA fragments that encoded a catalytic domain-containing segment of rADAMTS-7 (aa 217-427) were subcloned into the *BamHI/XhoI* site. The primer sequences were sense: 5'-CGCGGATCCTCAATCAGCAAAGAGAAGTG-3', and antisense: 5'-CCGCTCGAGGGACGGTCATCTAAGCACAG-3'. Purified hTSP-1 was incubated with the bacteria-expressed catalytic domain of ADAMTS-7 in a digestion buffer (50 mM Tris-HCl, 100 mM NaCl, 5 mM $CaCl_2$, 2 mM $ZnCl_2$, and 0.05% Brij-35, pH 7.5) at 37°C for 4 h[12].

Isolation of the mouse aortic ECs and VSMCs.

After PBS perfusion, the mouse arteries were harvested and dissected longitudinally. Endothelium was carefully scraped in PBS and collected from 7 mice by centrifugation. The precipitate was resuspended with 60 μl lysis buffer. For VSMC isolation, media of the aorta were tore up and grinded in lysis buffer. Expression of TSP-1 was analyzed with Western blot.

Statistical Analysis

All results were expressed as the mean ± standard error of the mean (SEM). Statistical analysis involved the use of Mann-Whitney U test for comparison of two groups to evaluate the effects of ADAMTS-7 on the BrdU incorporation, cell proliferation, and TSP-1 concentration by ELISA analysis in cell condition medium, to analyze the role of COMP on HUVEC proliferation, to assess the postinjury neointima area in WT and *comp*$^{-/-}$ mice. Comparisons among more than 2 groups involved non-parametric Kruskal-Wallis test with a

Dunn's post-hoc test to evaluate the effects of ADAMTS-7 neutralization antibody on cell proliferation and migration. Comparison of more than 2 groups involved two-way ANOVA followed by the Bonferroni test for post-hoc comparison as appropriate to evaluate the effects of ADAMTS-7 on re-endothelialization, neointima formation, the cell cycle and cell migration, as well as the effect of TSP-1 on ADAMTS-7 mediated cell proliferation, migration and re-endothelialization. Statistical analyses involved the use of GraphPad Prism 6.0 (GraphPad Software Inc, La Jolla, CA). All *P* -values were two-sided and a $P<0.05$ was considered statistically significant.

Supplemental Table 1. Large-scale phenotyping of the *Adamts7*$^{-/-}$ mouse (in cooperation with the German Mouse Clinic).

Screens	Phenotype of *Adamts7*$^{-/-}$-mice
Behaviour	Decreased anxiety in open field test
Neurology	Reduced rotarod latency in females
Nociception	None
Dysmorphology	None
Clinical Chemistry	*Mild effects on triglycerides and red blood cell count*
Energy Metabolism	*Increased maximum oxygen consumption in males*
Cardiovascular	*None*
Eye	None
Immunology	None
Allergy	None
Steroid Metabolism	None
Lung function	Increase in lung function parameters, reduced resistance
Pathology	*None*

Supplemental Table 1

Supplemental Table 2. Phenotyping of *Adamts7*$^{-/-}$ mice (KO) compared to WT mice regarding energy metabolism, clinical chemistry and hematology. Data are mean ± SD.

Test	Female		Male		Linear model		
					sex	genotype	sex:genotype
Energy metabolism	**WT (n=7)**	**KO (n=8)**	**WT (n=7)**	**KO (n=8)**			
Avg. mass [g]	21.8 ± 2.2	21.3 ± 1.1	28.1 ± 1	28.3 ± 1.6	<0.001	0.77	0.556
Food intake [g]	1.8 ± 0.7	1.4 ± 0.8	2.1 ± 0.7	2.4 ± 0.5	0.571	0.996	0.176
Max. VO2 [ml/(h animal)]	115.57 ± 18.14	117.88 ± 9.42	119.86 ± 7.36	134.63 ± 16.14	0.002	0.014	0.261
Avg. distance [cm]	5928 ± 1270	6532 ± 1983	4837 ± 3106	4576 ± 1624	0.057	0.824	0.577
Clinical chemistry	**WT (n=15)**	**KO (n=14)**	**WT (n=10)**	**KO (n=15)**			
Fasting glucose [mM]	5.79 ± 0.75	6.3 ± 0.86	6.63 ± 0.86	7.16 ± 1.37	0.002	0.056	0.965
Creatinine [µM]	10.43 ± 1.57	91.3 ± 2.7	9.65 ± 1.37	10.99 ± 1.42	0.298	0.973	0.013
Triglycerides [mM]	0.98 ± 0.28	0.86 ± 0.17	1.80 ± 0.31	1.49 ± 0.26	<0.001	0.003	0.177
Cholesterol [mM]	1.77 ± 0.26	1.69 ± 0.21	2.03 ± 0.28	1.98 ± 0.30	<0.001	0.377	0.818
ALP [U/l]	146 ± 15	157 ± 11	84 ± 8	83 ± 10	<0.001	0.137	0.06
Hematology	**WT (n=15)**	**KO (n=14)**	**WT (n=10)**	**KO (n=15)**			
RBC [10^6/mm^3]	10.85 ± 0.24	10.58 ± 0.39	10.77 ± 0.22	10.62 ± 0.36	0.844	0.02	0.503
HGB [g/dl]	16.51 ± 0.29	15.96 ± 0.53	16.13 ± 0.39	15.95 + 0.48	0.105	0.004	0.139
WBC [10^3/mm^3]	7.55 ± 2.04	6 ± 0.88	7.65 ± 1.5	8.79 ± 1.52	0.001	0.635	0.003
PLT [10^3/mm^3]	1281.6 ± 106.47	1316.79 ± 97.55	1331.8 ± 113.71	1291.6 ± 201.71	0.746	0.948	0.331

Supplemental Table 3. Phenotyping of *Adamts7*$^{-/-}$ mice (KO) compared to WT mice regarding pulmonary function. Data are mean [CI].

Test	Female WT n=5	Female KO n=6	p-value
Tidal volume, ml	0.22 [0.22-0.22]	0.23 [0.23-0.24]	0.011
Vital capacity, ml	0.98 [0.91-1.16]	1.23 [1.19-1.50]	0.061
Funct. residual capacity, ml	0.25 [0.23-0.25]	0.32 [0.28-0.36]	0.024
Residual volume, ml	0.015 [0.008-0.02]	0.025 [0.015-0.0.033]	0.4
Total lung capacity, ml	0.96 [0.89-1.17]	1.26 [1.16-1.39]	0.052
Forced vital capacity, ml	0.89 [0.81-1.08]	1.24 [1.05-1.43]	0.19
Forced exspiratory volume, ml	0.87 [0.79-1.04]	1.195 [1.035-1.35]	0.111
Dynamic lung compliance, ml/cmH_2O	0.02 [0.02-0.02]	0.03 [0.03-0.03]	0.015
Lung resistance, cmH_2O/ml/s	1.36 [1.34-1.39]	1.25 [1.22-1.29]	0.126

Supplemental Table 4. Blood lipid levels after 15 weeks of western diet comparing WT mice and *Adamts7*$^{-/-}$ mice (KO). Data are mean ± SD.

Test	**WT** **n=8**	**KO** **n=5**	**p-value**
Cholesterol, mmol/l	5.17 ± 1.81	4.83 ± 1.16	0.721
LDL-cholesterol, mmol/l	0.53 ± 0.19	0.52 ± 0.09	0.916
HDL-cholesterol, mmol/l	2.10 ± 0.53	2.06 ± 0.41	0.879
Triglycerides, mmol/l	0.58 ± 0.12	0.60 ± 0.15	0.790

Supplemental Table 5. Differentially expressed proteins in the conditioned media of Ad-*GFP* (G) and Ad-*ADAMTS-7* (T) SMCs.

Protein Name	UniProt ID	Mw	T-Test (*P*-Value)	Fold Change (T/G)	Normalized Spectral Count			Normalized Spectral Count		
					G1	G2	G3	T1	T2	T3
6-phosphogluconate dehydrogenase, decarboxylating	6PGD_RAT	53 kDa	0.00003	Infinite	0.0	0.0	0.0	5.5	6.4	6.4
A disintegrin and metalloproteinase with thrombospondin motifs 7	ATS7_RAT	176 kDa	0.00020	Infinite	0.0	0.0	0.0	152.9	189.0	150.2
Actin-related protein 3	ARP3_RAT	47 kDa	0.049	2.95	0.0	5.8	2.9	10.1	9.1	6.4
Alpha-actinin-1	ACTN1_RAT	103 kDa	0.016	1.41	30.5	34.9	30.7	45.1	50.2	40.1
Alpha-actinin-4	ACTN4_RAT	105 kDa	0.030	1.29	31.7	38.4	37.4	44.2	51.1	43.7
Elastin	ELN_RAT	73 kDa	0.048	-1.90	79.3	78.0	51.8	51.6	32.0	26.4
Elongation factor 2	EF2_RAT	95 kDa	0.027	2.26	4.9	4.7	3.8	12.9	10.0	7.3
Growth/differentiation factor 6	GDF6_RAT	51 kDa	0.017	-Infinite	8.5	4.7	3.8	0.0	0.0	0.0
Guanine nucleotide-binding protein subunit beta-2-like 1	GBLP_RAT	35 kDa	0.019	6.75	2.4	0.0	0.0	4.6	7.3	4.6
Heterogeneous nuclear ribonucleoprotein K	HNRPK_RAT	51 kDa	0.0010	Infinite	0.0	0.0	0.0	4.6	6.4	4.6
Heterogeneous nuclear ribonucleoprotein Q	HNRPQ_RAT	60 kDa	0.0020	Infinite	0.0	0.0	0.0	3.7	3.7	5.5
Importin subunit beta-1	IMB1_RAT	97 kDa	0.031	Infinite	0.0	0.0	0.0	2.8	6.4	2.7
Low molecular weight phosphotyrosine protein phosphatase	PPAC_RAT	18 kDa	0.031	Infinite	0.0	0.0	0.0	2.8	6.4	2.7
Moesin	MOES_MOUSE	68 kDa	0.0065	2.18	8.5	7.0	6.7	13.8	19.2	15.5
Olfactomedin-like protein 3	OLFL3_RAT	46 kDa	0.046	-1.56	7.3	9.3	7.7	6.4	3.7	5.5
Osteopontin	OSTP_RAT	35 kDa	0.023	-5.80	20.7	17.5	9.6	2.8	5.5	0.0
Periostin	POSTN_MOUSE	93 kDa	0.023	-1.60	34.2	32.6	32.6	21.2	14.6	26.4
Peroxiredoxin-5, mitochondrial	PRDX5_RAT	22 kDa	0.040	5.95	0.0	0.0	3.8	5.5	11.0	6.4
Pigment epithelium-derived factor	PEDF_MOUSE	46 kDa	0.0066	-1.49	32.9	31.4	29.7	19.3	19.2	24.6
Proliferation-associated protein 2G4	PA2G4_MOUSE	44 kDa	0.00064	Infinite	0.0	0.0	0.0	3.7	2.7	2.7
Protein DJ-1	PARK7_RAT	20 kDa	0.0057	Infinite	0.0	0.0	0.0	4.6	2.7	2.7
Pyruvate kinase isozymes M1/M2	KPYM_RAT	58 kDa	0.030	2.13	7.3	9.3	18.2	24.9	28.3	20.9
Septin-11	SEP11_RAT	50 kDa	0.012	7.94	0.0	0.0	2.9	6.4	6.4	10.0
Sushi repeat-containing protein SRPX	SRPX_RAT	52 kDa	0.018	-1.92	8.5	11.6	9.6	5.5	3.7	6.4
Sushi, von Willebrand factor type A, EGF and pentraxin domain-containing protein 1	SVEP1_RAT	387 kDa	0.0027	-8.51	4.9	5.8	4.8	0.0	0.0	1.8
T-complex protein 1 subunit theta	TCPQ_MOUSE	60 kDa	0.0014	Infinite	0.0	0.0	0.0	5.5	5.5	3.6
Thioredoxin	THIO_RAT	12 kDa	0.027	3.04	0.0	4.7	2.9	8.3	8.2	6.4
Thrombospondin-1	TSP1_MOUSE	130 kDa	0.05	-1.32	111.0	115.3	88.3	72.8	78.5	86.5
Ubiquitin carboxyl-terminal hydrolase 5	UBP5_HUMAN	96 kDa	0.0066	Infinite	0.0	0.0	0.0	2.8	3.7	1.8

Supplemental Table 6. Primer sequences of rat ADAMTS-7 (rTS7) fragments for mammalian two-hybrid.

Primer	Sequence(5'to3')
rTS7(26-246) forward	ACGGTCGACTTCCAACTGAGGGCCGGGCGGGTTTG
rTS7(26-246) reverse	TGCTCTAGAGCTCTCCACTTGCGGCTGCCCGTGGTA
rTS7(238-711) forward	ACGGTCGACTTTACCACGGGCAGCCGCAAGTGGAG
rTS7(238-711) reverse	TGCTCTAGACTCCTCAATGAGAATCTCTCGGGCTCC
rTS7(703-1007) forward	ACGGTCGACTTGGAGCCCGAGAGATTCTCATTGAG
rTS7(703-1007) reverse	TGCTCTAGAGACCGGCTGGTGCGGGTCGAAGTCAAC
rTS7(999-1595) forward	GCAGATATCAGTTGACTTCGACCCGCACCAGCCG
rTS7(999-1595) reverse	TGCTCTAGAGGGACATGAGCGGCAGCACTGAGCGCG

Supplemental Table 6

Supplemental Figures and Figure Legends

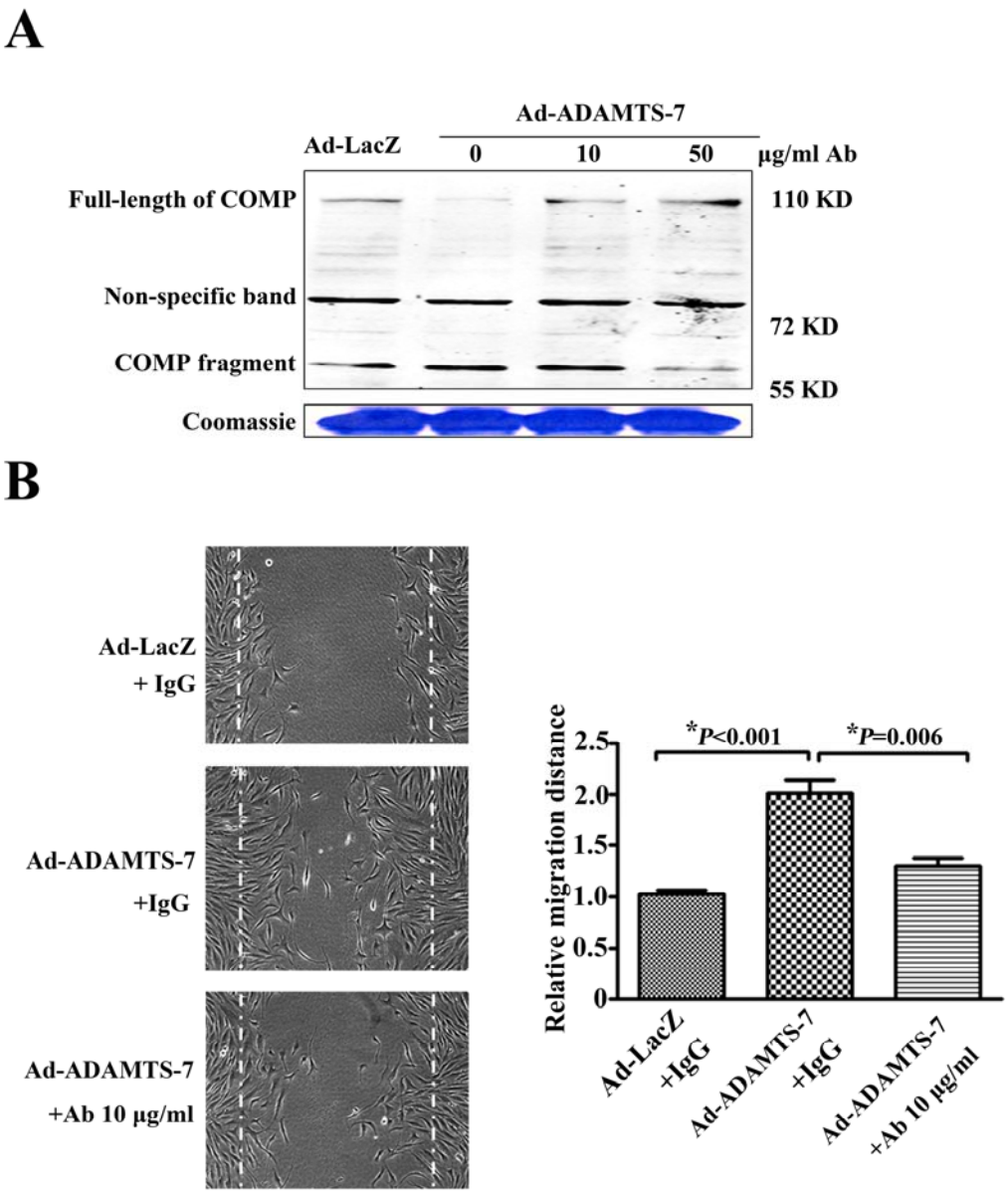

Supplemental Figure 1

Supplemental Figure 1. Characterization of ADAMTS-7 neutralization antibody.

(A) Representative Western Blot analysis of COMP cleavage. COMP-stable transfected 293A cell were infected by Ad-ADAMTS-7, followed by increasing amount of ADAMTS-7

neutralization antibody. Full-length COMP band (110 KD under reducing condition) and a COMP fragment (≈55 KD) were detected. (B) Representative images of HA VSMC migration after scratch would injury in the presence or absence of ADAMTS-7 neutralization antibody. The mean distance migrated by VSMCs was quantified. Results are means±SEM from 3 independent experiments, **P*<0.05. Magnification is ×100.

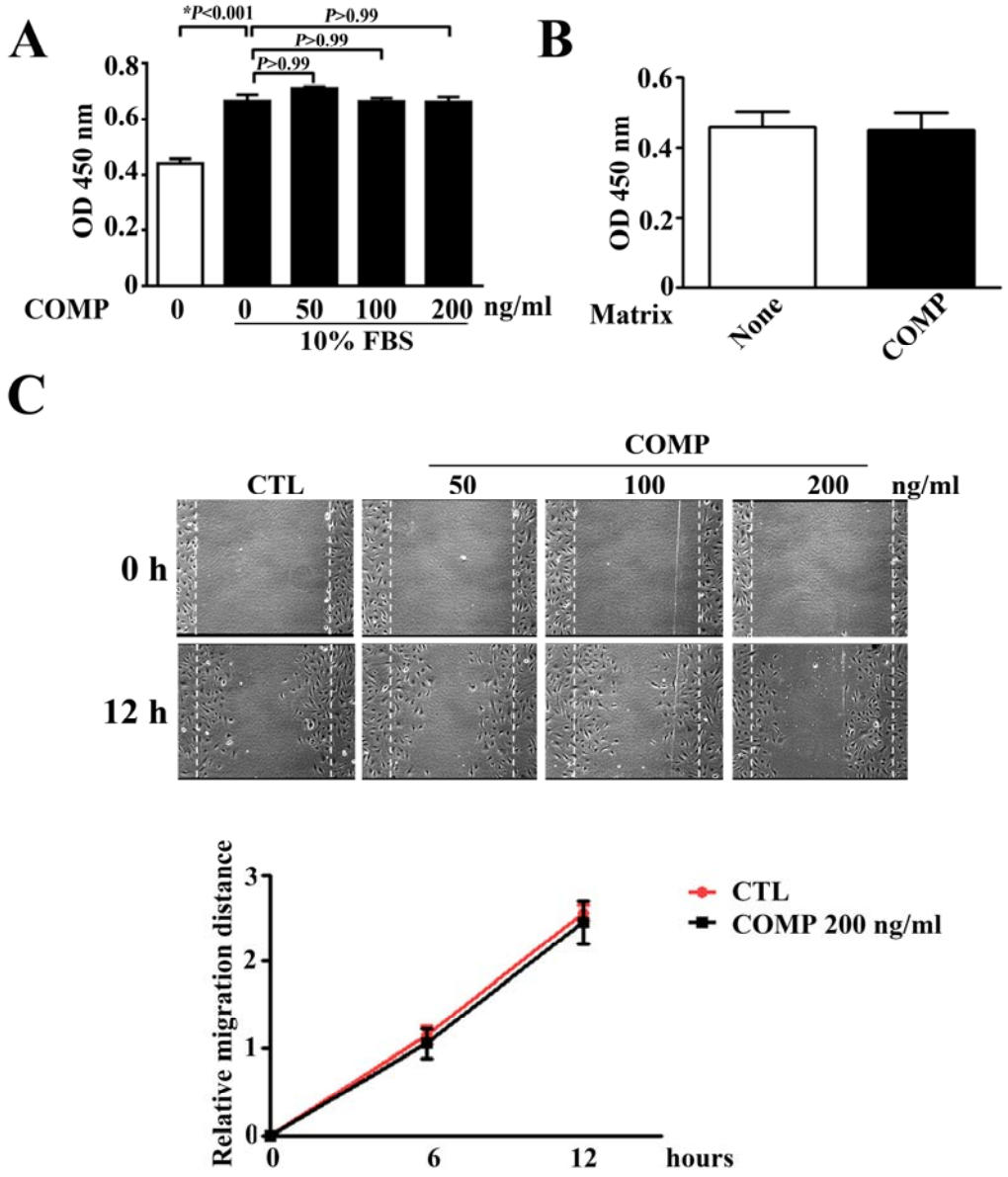

Supplemental Figure 2

D

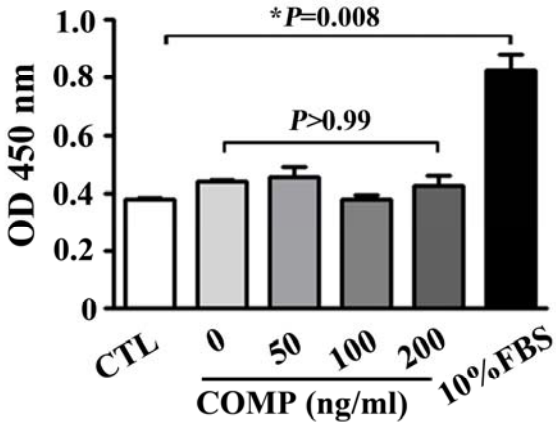

E

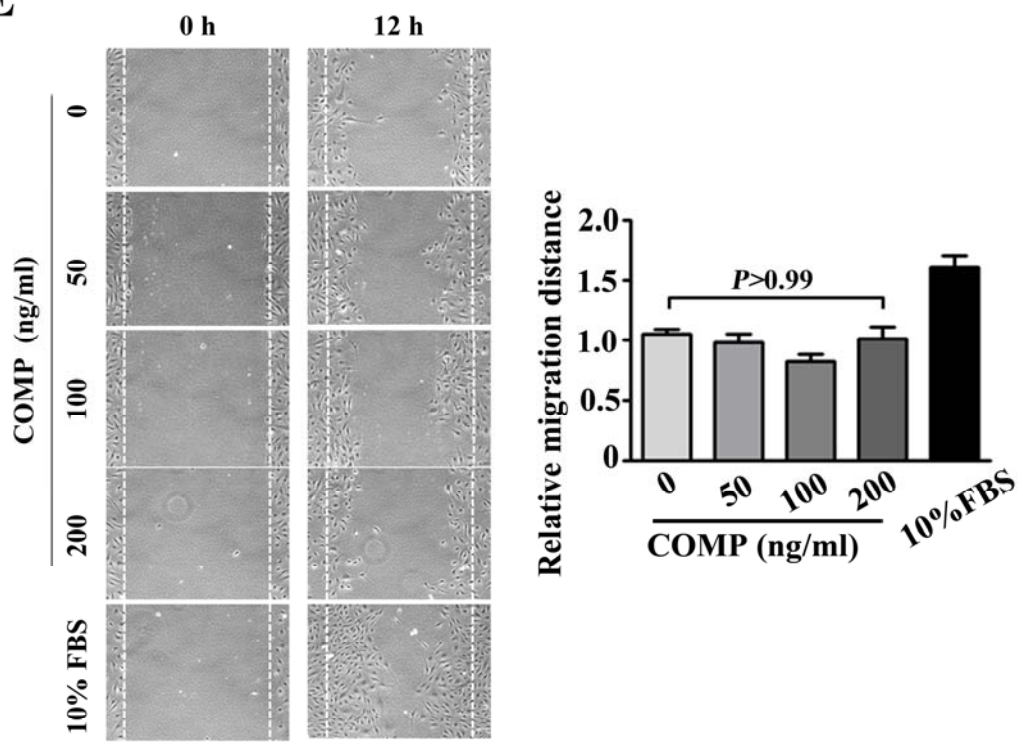

Supplemental Figure 2 continued

F

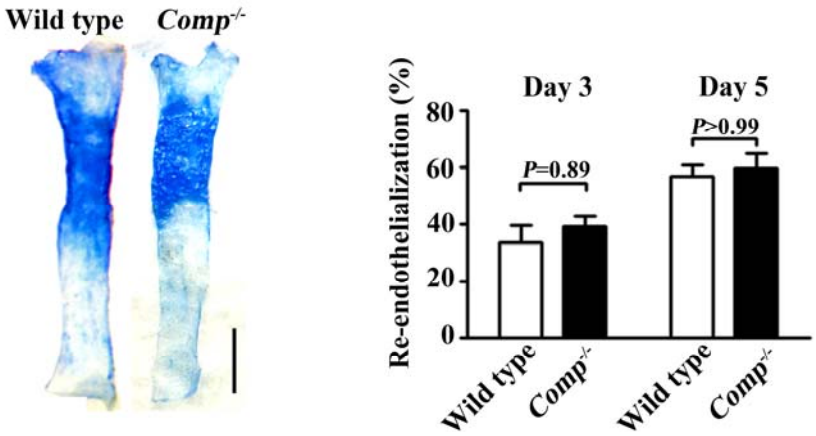

Supplemental Figure 2 continued 2

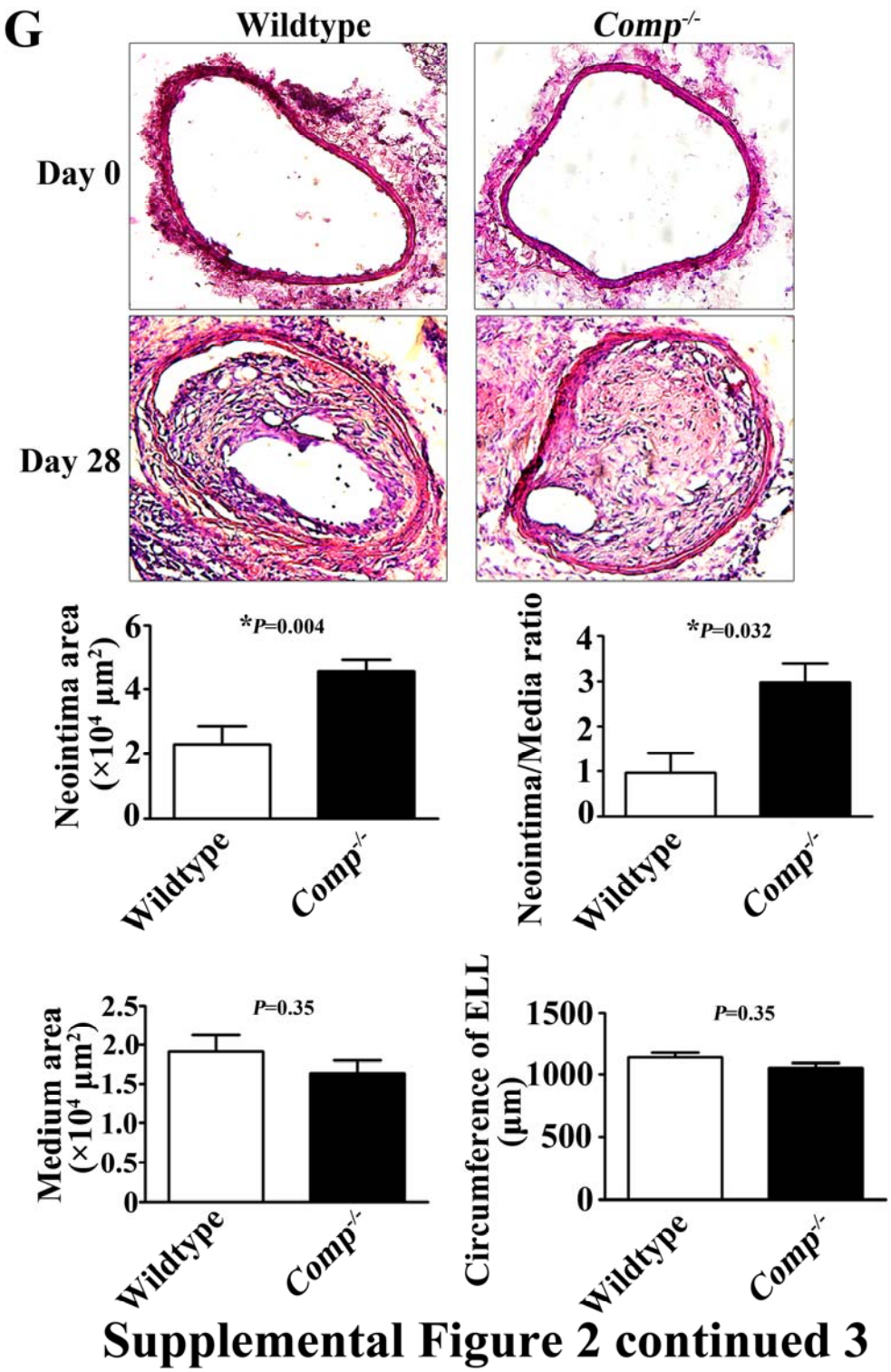

Supplemental Figure 2 continued 3

Supplemental Figure 2. Effects of COMP on HUVEC proliferation and migration.

(A) Proliferation of HUVECs with COMP supplement in culture medium via cell counting kit-8. Results are means±SEM from 3 independent experiments performed in duplicate. (B)

HUVECs were cultured on a plate coated with or without COMP protein (30 μg/ml). Cell proliferation was analyzed 24 hours after synchronization. Results are means±SEM from 3 independent experiments. (C) Representative images of cell migration after scratch in COMP-treated HUVECs. The mean distance was quantified. Results are means±SEM from 3 independent experiments. Magnification was ×100. (D&E) Proliferation and migration of HUVECs with COMP under 1% FBS. 10% FBS was a positive control. Results were means±SEM from 3 independent experiments, **P*<0.05. (F) Representative pictures of Evans blue stained carotid arteries 3 or 5 days after vascular injury. Scar bar, 1 mm. n=6-8 for each group. (G) Neointima formation was determined on hematoxylin and eosin–stained cross sections of carotid arteries 0 day and 28 days after vascular wire injury in wild type and *Comp*$^{-/-}$ mice (n=6 each group). Scar bar, 100 μm. **P*<0.05.

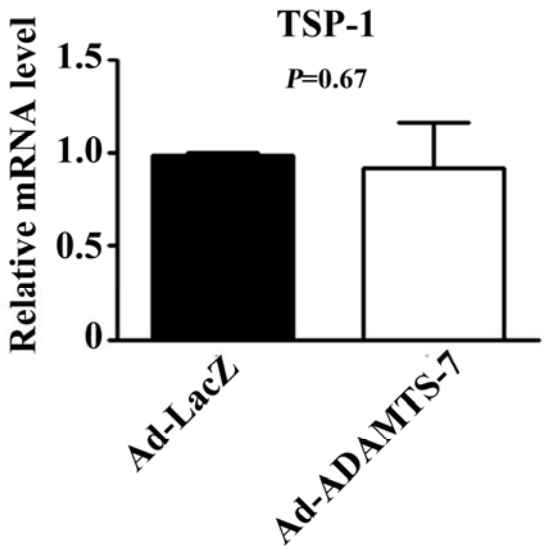

Supplemental Figure 3

Supplemental Figure 3. mRNA level of TSP-1 in Ad-*ADAMTS-7*-infected or Ad-*LacZ*-infected HUVECs. Results are means±SEM from 5 independent experiments.

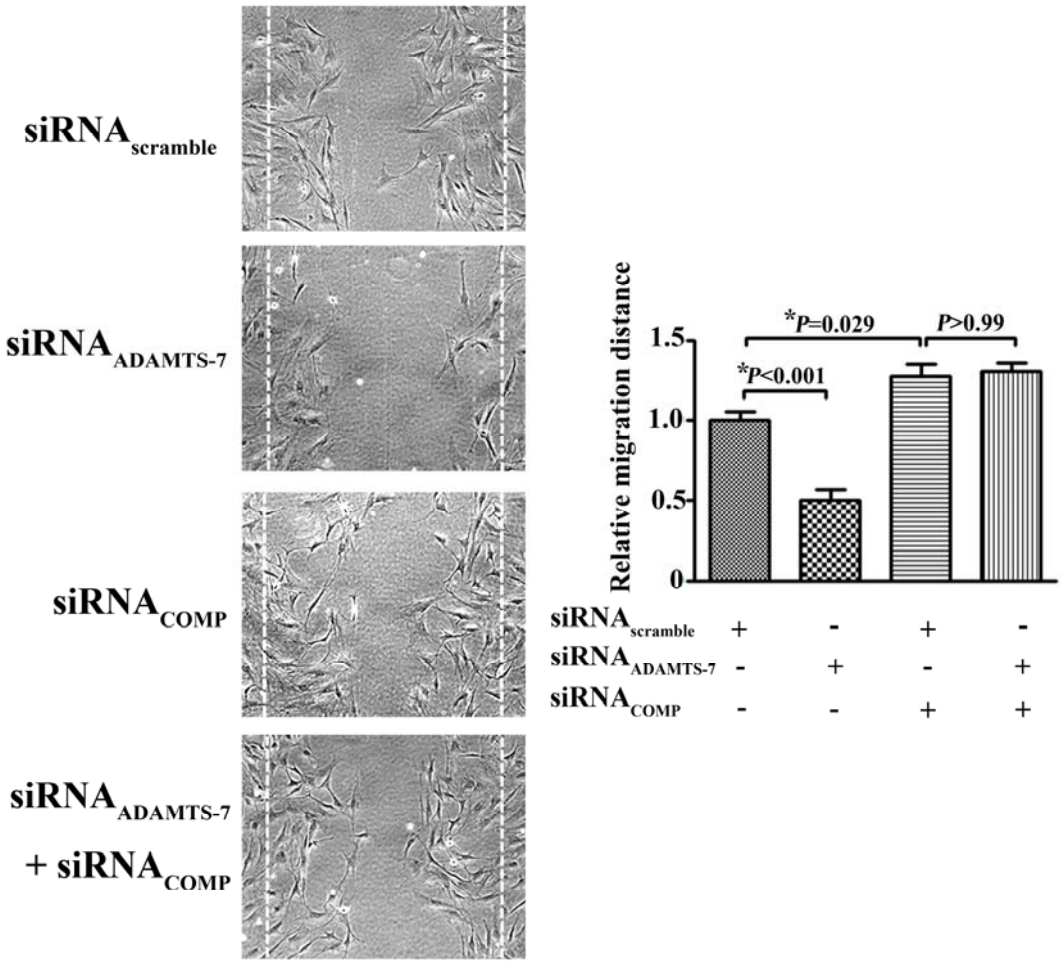

Supplemental Figure 4

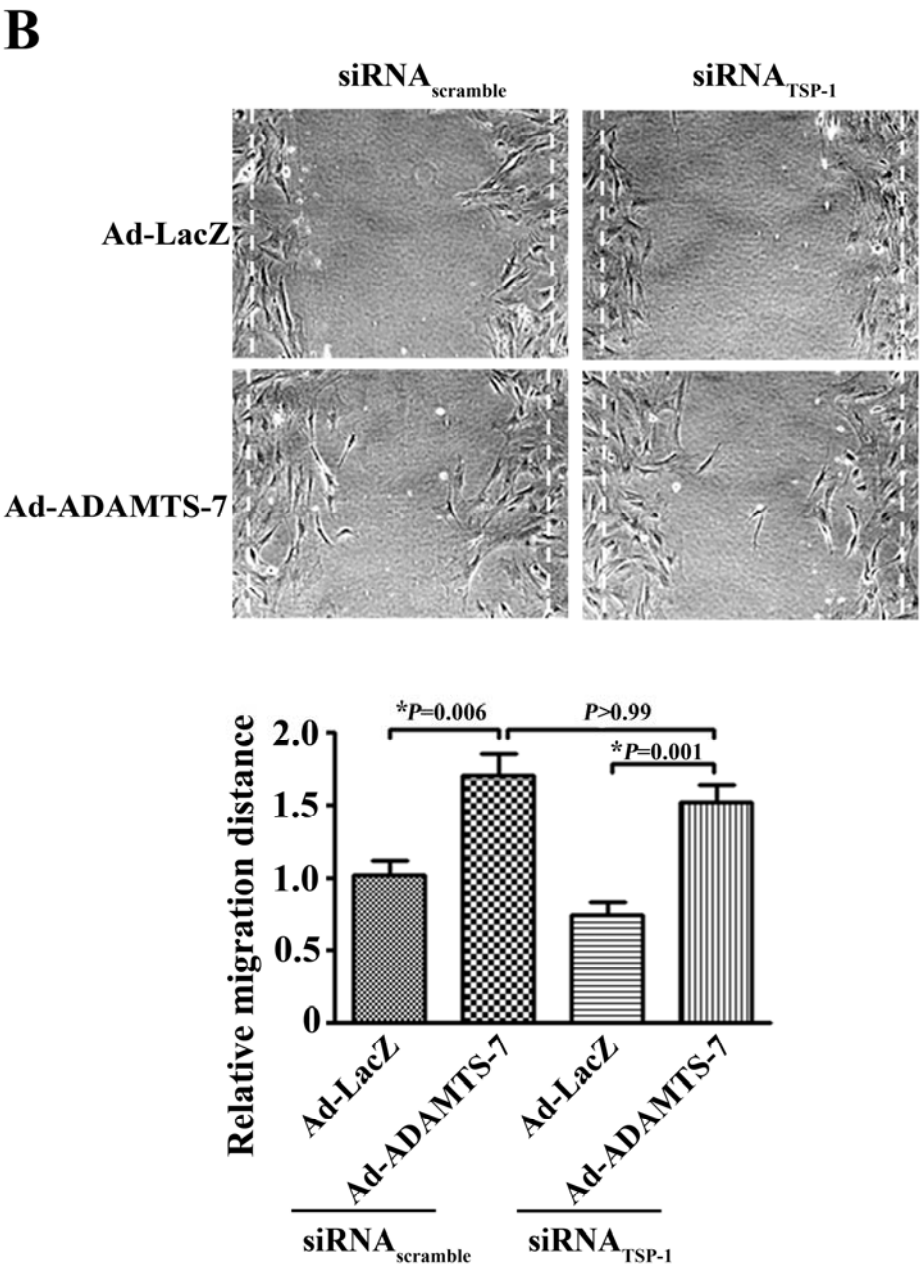

Supplemental Figure 4 continued

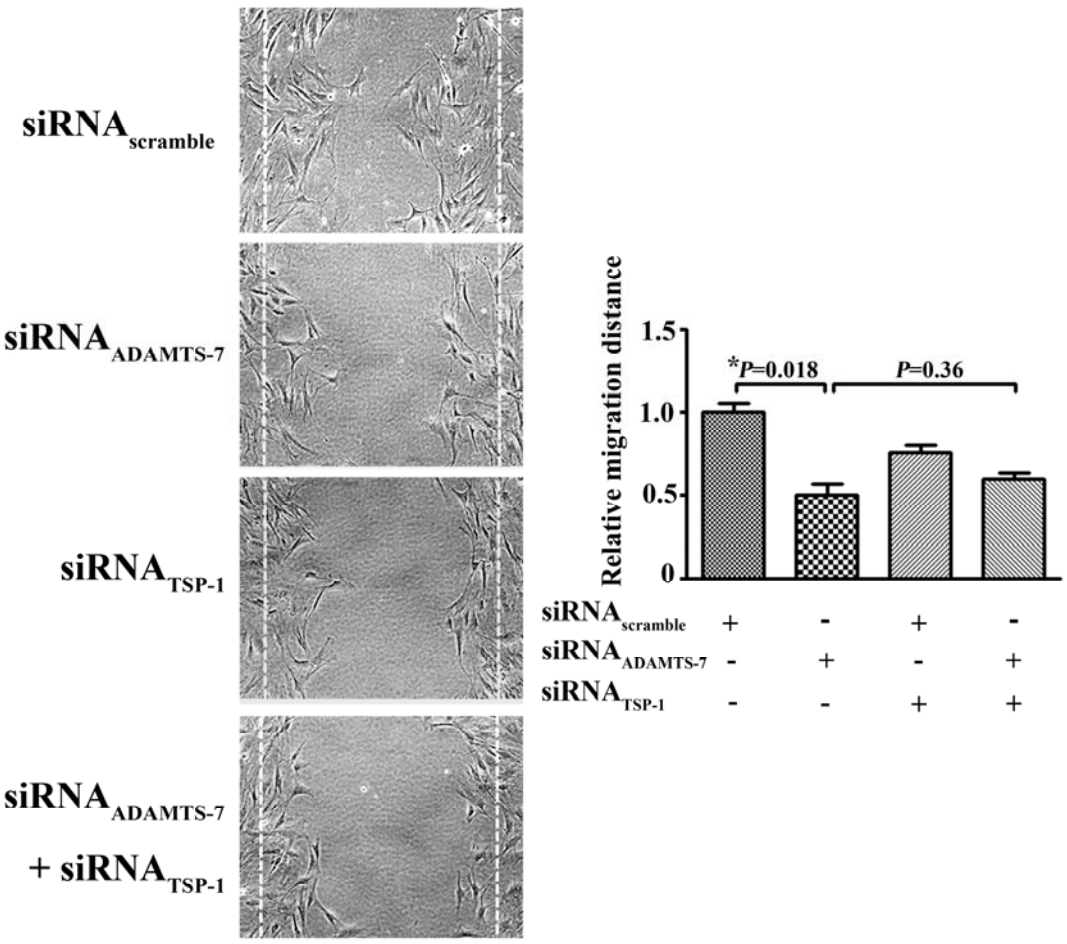

Supplemental Figure 4 continued 2

Supplemental Figure 4. ADAMTS-7 mediates VSMCs migration via COMP but not TSP-1. (A) Representative images of cell migration 12 hours after scratch in specific siRNA-treated rat VSMCs. Magnification was ×100. (B&C) Effect of ADAMTS-7 overexpression/silencing on cell migration in TSP-1 siRNA-treated rat VSMCs.

Magnification was ×100. The mean distance was quantified. Results are means±SEM from 3 independent experiments, *P<0.05.

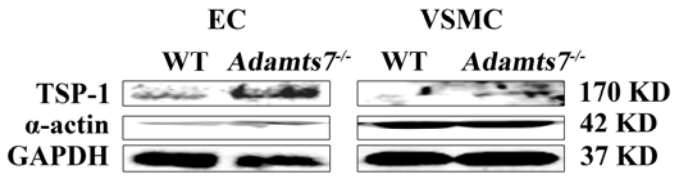

Supplemental Figure 5

Supplemental Figure 5. Protein expression of TSP-1 in EC and VSMC from wildtype (WT) and *Adamts7*$^{-/-}$ aorta respectively.

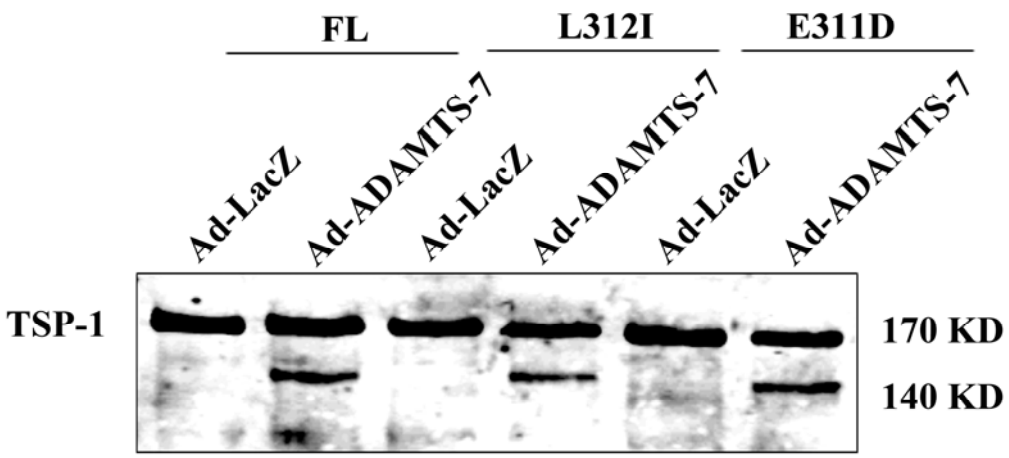

Supplemental Figure 6

Supplemental Figure 6. Western blot of TSP-1 cleaved by ADAMTS-7, mutant ADAMTS-7 L312I and E311D.

Reference

1. Friedel RH, Seisenberger C, Kaloff C, Wurst W. Eucomm--the european conditional mouse mutagenesis program. *Brief Funct Genomic Proteomic*. 2007;6:180-185.

2. Austin CP, Battey JF, Bradley A, Bucan M, Capecchi M, Collins FS, Dove WF, Duyk G, Dymecki S, Eppig JT, Grieder FB, Heintz N, Hicks G, Insel TR, Joyner A, Koller BH, Lloyd KC, Magnuson T, Moore MW, Nagy A, Pollock JD, Roses AD, Sands AT, Seed B, Skarnes WC, Snoddy J, Soriano P, Stewart DJ, Stewart F, Stillman B, Varmus H, Varticovski L, Verma IM, Vogt TF, von Melchner H, Witkowski J, Woychik RP, Wurst W, Yancopoulos GD, Young SG, Zambrowicz B. The knockout mouse project. *Nat Genet*. 2004;36:921-924.

3. Gailus-Durner V, Fuchs H, Becker L, Bolle I, Brielmeier M, Calzada-Wack J, Elvert R, Ehrhardt N, Dalke C, Franz TJ, Grundner-Culemann E, Hammelbacher S, Holter SM, Holzlwimmer G, Horsch M, Javaheri A, Kalaydjiev SV, Klempt M, Kling E, Kunder S, Lengger C, Lisse T, Mijalski T, Naton B, Pedersen V, Prehn C, Przemeck G, Racz I, Reinhard C, Reitmeir P, Schneider I, Schrewe A, Steinkamp R, Zybill C, Adamski J, Beckers J, Behrendt H, Favor J, Graw J, Heldmaier G, Hofler H, Ivandic B, Katus H, Kirchhof P, Klingenspor M, Klopstock T, Lengeling A, Muller W, Ohl F, Ollert M, Quintanilla-Martinez L, Schmidt J, Schulz H, Wolf E, Wurst W, Zimmer A, Busch DH, de Angelis MH. Introducing the german mouse clinic: Open access platform for standardized phenotyping. *Nat Methods*. 2005;2:403-404.

4. Fuchs H, Gailus-Durner V, Adler T, Aguilar-Pimentel JA, Becker L, Calzada-Wack J, Da Silva-Buttkus P, Neff F, Gotz A, Hans W, Holter SM, Horsch M, Kastenmuller G,

Kemter E, Lengger C, Maier H, Matloka M, Moller G, Naton B, Prehn C, Puk O, Racz I, Rathkolb B, Romisch-Margl W, Rozman J, Wang-Sattler R, Schrewe A, Stoger C, Tost M, Adamski J, Aigner B, Beckers J, Behrendt H, Busch DH, Esposito I, Graw J, Illig T, Ivandic B, Klingenspor M, Klopstock T, Kremmer E, Mempel M, Neschen S, Ollert M, Schulz H, Suhre K, Wolf E, Wurst W, Zimmer A, Hrabe de Angelis M. Mouse phenotyping. *Methods*. 2011;53:120-135.

5. Lindner V, Fingerle J, Reidy MA. Mouse model of arterial injury. *Circ res*. 1993;73:792-796.

6. Tan H, Jiang X, Yang F, Li Z, Liao D, Trial J, Magera MJ, Durante W, Yang X, Wang H. Hyperhomocysteinemia inhibits post-injury reendothelialization in mice. *Cardiovasc Res*. 2006;69:253-262.

7. Grote K, Sonnenschein K, Kapopara PR, Hillmer A, Grothusen C, Salguero G, Kotlarz D, Schuett H, Bavendiek U, Schieffer B. Toll-like receptor 2/6 agonist macrophage-activating lipopeptide-2 promotes reendothelialization and inhibits neointima formation after vascular injury. *Arterioscler Thromb Vasc Biol*. 2013;33:2097-2104.

8. Bai X, Margariti A, Hu Y, Sato Y, Zeng L, Ivetic A, Habi O, Mason JC, Wang X, Xu Q. Protein kinase cδ deficiency accelerates neointimal lesions of mouse injured artery involving delayed reendothelialization and vasohibin-1 accumulation. *Arterioscler Thromb Vasc Biol*. 2010;30:2467-2474.

9. Zheng S, Li W, Xu M, Bai X, Zhou Z, Han J, Shyy JY-J, Wang X. Calcitonin gene-related peptide promotes angiogenesis via amp-activated protein kinase. *Am J*

Physiol Cell Physiol. 2010;299:C1485-C1492.

10. Yin X, Bern M, Xing Q, Ho J, Viner R, Mayr M. Glycoproteomic analysis of the secretome of human endothelial cells. *Mol Cell Proteomics*. 2013;12:956-978.

11. Lee NV, Sato M, Annis DS, Loo JA, Wu L, Mosher DF, Iruela-Arispe ML. Adamts1 mediates the release of antiangiogenic polypeptides from tsp1 and 2. *EMBO J*. 2006;25:5270-5283.

12. Liu C-j, Kong W, Ilalov K, Yu S, Xu K, Prazak L, Fajardo M, Sehgal B, Di Cesare PE. Adamts-7: A metalloproteinase that directly binds to and degrades cartilage oligomeric matrix protein. *The FASEB journal*. 2006;20:988-990.

APPENDIX X:

[§]German Mouse Clinic, Helmholtz Zentrum München, German Research Center for Environmental Health GmbH, Neuherberg, Germany

Thure Adler [1,2]

Dirk H. Busch [2]

Antonio Aguilar-Pimentel[1,3]

Markus Ollert[3, 11]

Oana Amarie[1,4]

Tobias Stoeger[1,4]

Ali Önder Yildrim[1,4]

Oliver Eickelberg[4]

Cornelia Prehn[1]

Jerzy Adamski[1]

Lore Becker[1,5]

Alexandra Vernaleken[1, 5]

Thomas Klopstock [5,16,20,21]

Marion Horsch[1]

Johannes Beckers[1,18,19]

Kristin Moreth[1]

Raffi Bekeredjian[6]

Hugo Katus[6]

Lillian Garrett[1,8]

Sabine M. Hölter [1,8]

Annemarie Zimprich[1,8]

Wolfgang Wurst [8,14,15,16,17,21]

Oliver Puk[1,8]

Jochen Graw [8]

Wolfgang Hans[1]

Jan Rozman [1,19]

Martin Klingenspor[9,10]

Laura Brachthäuser[1,7]

Julia Calzada-Wack[1,7]

Dirk Janik[1,7]

Tanja Klein-Rodewald[1,7]

Frauke Neff[1,7]

Ildikó Rácz[1,12]

Andreas Zimmer[12]

Birgit Rathkolb [1,13,19]

Eckhard Wolf [13]

Manuela Gegenfurtner[1]

Ralph Steinkamp[1]

Christoph Lengger[1]

Holger Maier[1]

Claudia Stoeger[1]

Stefanie Leuchtenberger[1]

Valérie Gailus-Durner [1]

Helmut Fuchs [1]

Martin Hrabě de Angelis [1,18,19]

1 German Mouse Clinic, Institute of Experimental Genetics, Helmholtz Zentrum München, German Research Center for Environmental Health GmbH, Ingolstaedter Landstrasse 1, 85764 Neuherberg, Germany

2 Institute for Medical Microbiology, Immunology and Hygiene, Technical University of Munich, Trogerstrasse 9, 81675 Munich, Germany

3 Department of Dermatology and Allergy, Biederstein, Klinikum rechts der Isar, Technische Universität München (TUM), Biedersteiner Str. 29, 80802 Munich,

4 Comprehensive Pneumology Center, Institute of Lung Biology and Disease, Helmholtz Zentrum München, German Research Center for Environmental Health (GmbH), Ingolstädter Landstraße 1, 85764 Neuherberg, Germany and Member of the German Center for Lung Research

5 Department of Neurology, Friedrich-Baur-Institut, Ludwig-Maximilians-Universität München, Ziemssenstrasse 1a, 80336 Munich, Germany

6 Department of Cardiology, University of Heidelberg, Im Neuenheimer Feld 410, 69120 Heidelberg, Germany

7 Institute of Pathology, Helmholtz Zentrum München, German Research Center for

Environmental Health GmbH, Ingolstaedter Landstrasse 1, 85764 Neuherberg, Germany

8 Institute of Developmental Genetics, Helmholtz Zentrum München, German Research Center for Environmental Health GmbH, Ingolstaedter Landstrasse 1, 85764 Neuherberg, Germany

9 Chair for Molecular Nutritional Medicine, Technische Universität München, Else Kröner-Fresenius Center for Nutritional Medicine, 85350 Freising, Germany

10 ZIEL – Center for Nutrition and Food Sciences, Technische Universität München, 85350 Freising, Germany

11 Clinical Research Group Molecular Allergology, Center of Allergy and Environment Munich (ZAUM), Technische Universität München (TUM), and Institute for Allergy Research, Helmholtz Zentrum München, German Research Center for Environmental Health, Neuherberg, Germany

12 Institute of Molecular Psychiatry, University of Bonn, Sigmund-Freud-Strasse 25, 53127 Bonn, Germany

13 Ludwig-Maximilians-Universität München, Gene Center, Institute of Molecular Animal Breeding and Biotechnology, Feodor-Lynen Strasse 25, 81377 Munich, Germany

14 Chair of Developmental Genetics, Center of Life and Food Sciences Weihenstephan, Technische Universität München, Ingolstaedter Landstrasse 1, 85764 Neuherberg, Germany

15 Max Planck Institute of Psychiatry, Kraepelinstr. 2-10 , 80804 Munich, Germany

16 Deutsches Institut für Neurodegenerative Erkrankungen (DZNE) Site Munich, Schillerstrasse 44, 80336 Munich, Germany

17 Munich Cluster for Systems Neurology (SyNergy), Adolf-Butenandt-Institut, Ludwig-Maximilians-Universität München, Schillerstrasse 44, 80336 Munich, Germany

18 Chair of Experimental Genetics, Center of Life and Food Sciences Weihenstephan, Technische Universität München, Ingolstaedter Landstrasse 1, 85764 Neuherberg, Germany

19 Member of German Center for Diabetes Research (DZD), Ingolstaedter Landstraße 1, 85764 Neuherberg, Germany

20 German Network for Mitochondrial Disorders (mitoNET)

21 German Center for Vertigo and Balance Disorders, Munich, Germany

ADAMTS-7 Inhibits Re-endothelialization of Injured Arteries and Promotes Vascular Remodeling Through Cleavage of Thrombospondin-1

Thorsten Kessler, Lu Zhang, Ziyi Liu, Xiaoke Yin, Yaqian Huang, Yingbao Wang, Yi Fu, Manuel Mayr, Qing Ge, Qingbo Xu, Yi Zhu, Xian Wang, Kjestine Schmidt, Cor de Wit, Jeanette Erdmann, Heribert Schunkert, Zouhair Aherrahrou and Wei Kong

Circulation. 2015;131:1191-1201; originally published online February 20, 2015;
doi: 10.1161/CIRCULATIONAHA.114.014072
Circulation is published by the American Heart Association, 7272 Greenville Avenue, Dallas, TX 75231

Print ISSN: 0009-7322. Online ISSN: 1524-4539